Using a Sinusoidal Water Temperature Signal to Relate Sediment Thermal Properties with Sediment Composition Within Streambeds

A Thesis

Presented in Partial Fulfillment of the Requirements for the

Degree of Master of Science

with a

Major in Civil Engineering

in the

College of Graduate Studies

University of Idaho

by

Aston M. Carpenter

Major Professor: Daniele Tonina, Ph.D., P.E.

Committee Members: Ralph Budwig, Ph.D., P.E.; Charles Luce, Ph.D.

Department Administrator: Patricia J. S. Colberg, Ph.D, P.E.

December 2020

AUTHORIZATION TO SUBMIT THESIS

This thesis of Aston M. Carpenter, submitted for the degree of Master of Science with a Major in Civil Engineering and titled "Using a Sinusoidal Water Temperature Signal to Relate Sediment Thermal Properties with Sediment Composition Within Streambeds," has been reviewed in the final form. Permission, as indicated by the signatures and dates below, is now granted to submit final copies to the College of Graduate Studies for approval.

Major Professor: _____ Date: _____

Daniele Tonina, Ph.D., P.E.

Committee Members: _____ Date: _____

Ralph Budwig, Ph.D., P.E.

_____ Date: _____

Charles Luce, Ph.D.

Department Administrator: _____ Date: _____

Patricia J. S. Colberg, Ph.D. P.E.

ABSTRACT

As our climate changes and urban sprawl continues, it is becoming increasingly important to quantify and track impacts on the environment. Rivers and streams are continuously changing due to high flows and sediment transport caused by both natural and anthropogenic phenomena. Specifically, scour and deposition both impact the structural stability of bridges, dams, and other structures, as well as influence the behaviors of fish and other organisms in rivers. This thesis tests a novel methodology to monitor streambed elevation changes and relates thermal properties of the sediment to sediment porosity based on daily variations in stream water temperature. The method uses one-dimensional heat advection and diffusion equations to determine streambed elevations. This method was able to monitor streambed elevation changes at bridge piers for over a year, with a maximum error of approximately 10 cm. The same method was used to determine thermal properties of the sediment, which may provide valuable insight into how thermal properties relate to sediment composition. Using this method in laboratory experiments, it was observed that as porosity is reduced, so is the thermal diffusivity of the substrate.

ACKNOWLEDGEMENTS

There are a number of people and organizations to whom I wish to show my gratitude. Without your invaluable assistance, this study would not have been possible. I would like to pay my special regards to my advisor and major professor Dr. Daniele Tonina for his much needed guidance and patience through the process of experimental design, data collection, and analysis, and the completion of this thesis. To Dr. Charles Luce, I would like to show my gratitude for his time and much needed technical support with this study, which cannot be easy given his busy schedule. Your expertise has helped pave and direct the analyses of this study. To Dr. Ralph Budwig for his time, expertise, and technical skills, which helped in the formation of this thesis. A special thanks to Tim DeWeese for his knowledge and mentorship to help me grow as a researcher and professional. Thanks also to Bob Basham, CER Stream lab Manager, who provided much needed expertise and help with the development, programming, and installation of experiment probes. The probes would not have been able to be deployed without his help. Thanks to Richie Carmichael for his valuable time and help on installation of experiment probes in the field.

The physical and technical contributions of the Idaho Transportation Department is truly appreciated. Without their support and funding, this study could not have reached its goals. I would finally like to give my sincere gratitude to the University of Idaho for the opportunity to perform research and extend my education at the Master's level.

I owe my deepest gratitude to my family, to whom I have dedicated this work. They have pushed me to grow not only as a person, but within my education and as a professional. I would like to thank you all for your patience and support throughout my entire education.

DEDICATION

To my mother and father, Theresa Modrick-Hansen and Matthew Carpenter, I dedicate this work to you as a thank you for all of the love, patience, and encouragement provided throughout my college education. To my sister, Mercedi Carpenter, for the much-needed support through the difficult times and keeping my spirits high. A special dedication to my wife, Sydney Carpenter, for supporting me throughout my program and pushing me to better myself in all aspects of my life. Without your support and sacrifices, this would not have been possible.

TABLE OF CONTENTSZ

LIST OF FIGURES

LIST OF TABLES

Chapter 1. A NOVEL TEMPERATURE-BASED MONITORING SYSTEM FOR SCOUR AND DEPOSITION AT BRIDGE PIERS

1.1 Introduction

Sediment transport can have many effects in fluvial environments. Depending on upstream conditions, sediment may be removed or deposited throughout the streambed impacting both the fluvial environment and structures within it. The removal of sediment, such as sand and gravel, (referred to as scour or local erosion), caused by swiftly flowing waters around structure foundations can hinder the stability of the structure leading to failure (Saito et al., 1990; Katsui and Toue, 1993; Sumer et al., 2001). A single flood event in 1993 in the Mississippi and Missouri river basins caused 22 of 28 bridges to fail due to scour (Kamojiala et al., 1994). The National Cooperative Highway Research Program (NCHRP) reported that 1,502 bridge failures occurring between 1966 and 2005 were the result of scour (Hunt, 2009). In a 30-year study done in 1995, approximately 60% of bridge collapses in the United Stated were caused by bridge scour, resulting in damage repair costs to highways estimated at $50 million per year (Richardson, 1999). A 15-year study completed in 2003 by the Federal Highway Administration (FHWA) identified over 26,000 bridges over waterways to be scour critical (Gee, 2003).

In Idaho, approximately 198 highway bridges are rated as scour-critical, meaning they are at risk of failure due to scour (ITD, 2004). Typically, measurements for scour are made during annual or bi-annual inspections. The Idaho Transportation Department (ITD) Scour Committee uses a proprietary alert system, Bridge Watch, for scour-critical bridges. Bridge Watch uses rain, snow, and stream gauge information to determine the probability of potential scour due to flow events. The Bridge Watch alert system does not measure scour but instead it predicts high flow events when scour is expected to be greatest. A request for inspection can then be issued to assess damage (ITD, 2015; 2016).

The most common way to monitor bridges is visual inspection (Prendergast et al., 2014). Divers and survey teams are used to inspect the condition of foundation elements and to measure the depth of scour using basic instrumentation (Avent and Alawady, 2005). This method is limited because the inspections cannot be carried out during times of high flows, when the risk of scour is at its highest. As water subsides from the flood event, scour holes may fill, and the maximum scour may

not be surveyed (Lin et al., 2010; Foti and Sabia, 2011; DeFalco and Mele, 2002). This may result insufficient data to determine the maximum scour that occurs.

Many different scour monitoring methods have been proposed to monitor scour and deposition at a higher frequency than bi-annually. Methods such as sonar, radar, time domain reflectometry, sliding collar, seismic, tilt and motion, float out devices, and magnetic fields have been used to monitor scour and deposition (Hunt 2009, Prendergast et al., 2014, Kenney and McKinney, Lee and Sturm, 2009, Yao et al., 2010, Hayden and Puleo, 2011, Fisher and Khan, 2013, Junliang et al., 2013, Chen et al., 2015).

Sonar and radar techniques contain attenuations and noise that result in complex signals and make it difficult to interpret important information. The noise in a signal is caused by a range of different phenomena including multiple channel reflections, echoes from the shoreline, bridge piers/abutments, sediment plumes, and bubbles (Hayden and Puelo, 2011; Anderson et al., 2007; Topczewski et al., 2016). There have been both two- and three-dimensional sonar systems designed to continuously monitor scour across a streambed (Hayden and Puelo, 2011; Topczewski et al., 2016). The accuracy of these sensors relies on the frequency emitted; higher frequencies are better for shorter distances, while lower frequencies are better for capturing depths over longer distances. Sonar methods may result in gaps in data where the signal cannot reach, for instance, areas around objects or dead zones in the center of a scour hole. Many of the acoustic tools used are large in size and require housing for protection (Hayden and Puelo, 2011). Having a housing set up on the side of a bridge pier is costly and may impede water flow, causing an unnatural flow event that may change the scour that occurs. Mounted sonar sensors are used to achieve near real-time monitoring of scour, while other sonar methods use boats that need to be guided across the river with measurements taken only periodically.

Ground Penetrating Radar (GPR) is another method used to measure scour. The GPR tool employs a coupled source antenna/receiver that produces a short period pulsed electromagnetic signal at a regular time or distance interval (Anderson et al., 2016). GPR has two- and three-dimensional capabilities that provide an accurate depth-structure model. Like sonar methods, GPR also has limits on the effective depth of a signal (Anderson et al., 2016; Nichol and Reynolds, 1999). Labor-intensive manual operation of GPR is required, preventing it from being used in real-time monitoring of scour (Horne, 1993; Forde et al., 1999; Webb et al., 2000).

Many methods, such as scour collars/chains, magnetic collars, radar, and magnetic field changes, are limited to point data collection rather than continuous data collection (Fisher and Khan, 2013; Chen et al., 2015; Anderson et al., 2007; Nichol and Reynolds, 1999; Web et al., 2000; Zarafshan et al., 2012). While features such as maximum scour can be obtained, patterns of scour may not be captured or understood. A high bridge failure rate caused by pier scouring events illustrates the importance of deploying real-time, continuous-scour monitoring systems (Fisher and Khan, et al. 2013; Zarafshan et al., 2012). Tao et al. (2013) present a time domain reflectometry (TDR) technique that demonstrates promise in monitoring scour changes in real-time. The TDR technique is based on guided electromagnetic wave technology that uses dielectric property mismatches to determine the water-sediment interface (Tao et al., 2013). A vibration-based technique has also proven to be applicable to real-time monitoring of bridge scour (Fisher and Khan, et al. 2013; Zarafshan et al., 2012). Zarafshan et al. (2012) describe the field application of a vibration-based method that tracks both scour and depositional events. None of the above real-time monitoring methods have an accuracy assessment, comparing data collected by the instruments with measured scour events.

Lotwick Reese, a hydraulic engineer and ITD project manager, explains, “Current methods for scour detection, which may include ring rods, acoustic or sonar technology, are too complicated or just impractical. Measurements of streambed elevation are difficult to obtain using current methods until after high flows have subsided; when flows subside, silt may be deposited, potentially masking a scour problem.” This research discusses a new temperature-based monitoring system called the thermal scour and deposition chain (TSDC). It was tested both in laboratory experiments and in preliminary field tests (Tonina et al, 2014; DeWeese, 2015) designed to assess scour and deposition.

The TSDC method uses naturally occurring diurnal temperature signal oscillations of stream waters. The amplitude and phase of a temperature signal changes as the signal propagates through the sediment (DeWeese, 2015); analysis of these changes reveals the thermal properties of the sediment (Tonina et al, 2014; DeWeese, 2015). Once the thermal property is quantified, it can be used along with the analysis of phase and amplitude derived from the one-dimensional heat diffusion-advection equation to quantify changes in bed elevation (Tonina et al., 2014). Tonina et al. (2014) applied the TSDC method in a small agricultural drainage channel, where large scour does not occur. Scour results obtained a root mean square error (RMSE) on the order of 1 cm or 20% error. DeWeese (2015) reported an average RMSE for bed elevation of 0.35 cm and a range of error from

0.70-8.90 cm for laboratory and field experiments, respectively. The TSDC method has not been applied directly to areas of high turbulence and varied flow.

This study is designed to validate the use of the TSDC for scour and deposition monitoring. To address this goal, five bridges were selected throughout Idaho. Each bridge is paired with either a maximum scour measurement or a monthly survey measurement of streambed elevation. One bridge was chosen as the control site, where no scour is expected; the other four bridges were selected because they are rated as scour critical.

1.1.1 Sites

The bridges used in this study were selected based on the following criteria: (1) presence of a USGS gauge station nearby; (2) accessibility; (3) observed scour/high-risk scour bridge; (4) low flows during installation; and (5) have at least one pier. The presence of a USGS gauge station is important because it allows a comparison of the time series of discharge, scour, and depositional events.

Banks Bridge, the control site, is located off Highway 55 on the North Fork of the Payette River near Banks, Idaho (Site a. Figure 1.1). The TSDC probe is located on the downstream end of the river right pier. Under the bridge and around the piers, the streambed is highly rip-rapped; therefore, no scour is expected to occur.

Pinehurst Bridge is located in northern Idaho on Pine Creek in Pinehurst, Idaho, just south of Interstate 90 (Site b. Figure 1.1). The bridge spans the width of the creek with one pier that is continuously in the water flow. On river left of the pier, water can become stagnant during low flows, while on river right of the pier water, flows throughout the year. One probe is located on each side of the pier where it was possible to drive the probe into the streambed. During installation, gravel was present on both sides of the pier with fine sediment filling in voids. Due to a narrow flow path, higher velocities were expected, which would result in a substantial amount of scour.

Pine Bridge is located in southeast Idaho near Pine, Idaho, on the South Fork of the Boise River as it enters Anderson Ranch Reservoir. It is a three-pier bridge (Site c. Figure 1.1). The middle pier was selected because of wadable waters during low flows. Two probes were installed at the river right of the middle pier, one on the upstream end and the second just past the center of the pier. At installation, the sediment composition was mainly fine sand and silt material. A gravel bar just upstream of the bridge has been migrating downstream toward the bridge. During site visits, the sediment material visibly changed from fine material to coarser gravel and cobbles. Streambed

bathymetric surveys were taken at this site approximately monthly to compare calculated with measured streambed elevations.

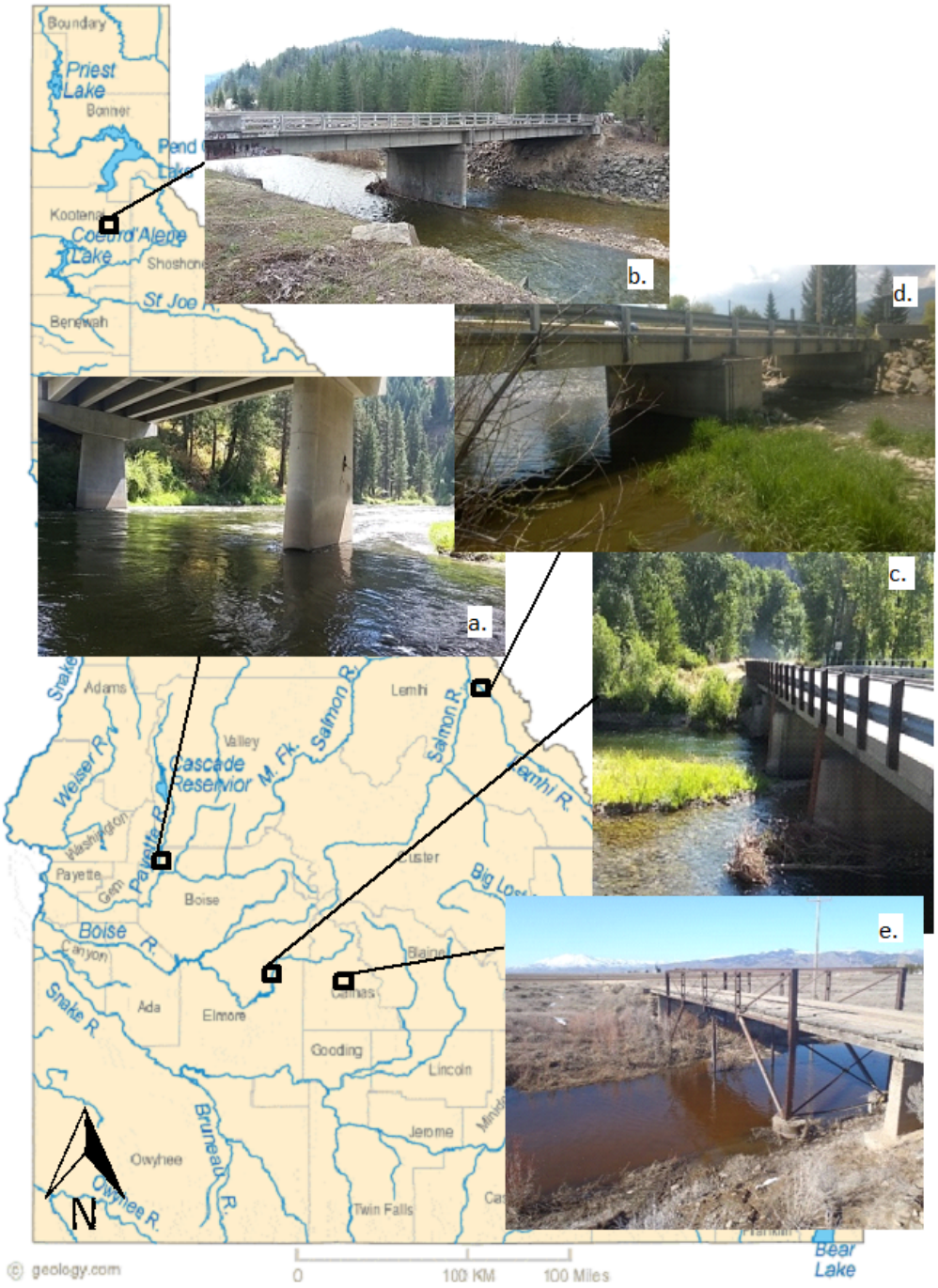

Figure 1.1. Project Site Locations

Salmon Bridge on the Lemhi River is located in the city of Salmon, Idaho (Site d. Figure 1.1). The bridge has one pier that is located roughly in the middle of the stream. Two probes are at the downstream end of the pier and placed approximately 10 feet apart. At installation, large gravel and cobbles were located below the bridge. Salmon Bridge was expected to have a minimal amount of scour due to the large grain sizes. Calculated scour was verified with maximum scour chain measurements.

Camas Creek Bridge is located on Camas Creek in Fairfield, Idaho (Figure 1.13). The bridge has three piers that extend into the streambed, but only one that remains in the main part of the flow throughout the year. One TSDC probe was located just upstream of the middle pier in the main part of the water flow. The Fairfield area has high agricultural use, which introduces a large amount of fine sediment into the creek. At the bridge location, sand and silt cover the creek bed, with bedrock just a few feet below the streambed surface. A large amount of scour and deposition was expected at this site, because of the fine sediment input from anthropogenic sources.

1.2 Methods

1.2.1 Theory

Changes in streambed elevation are quantified with analytical solutions based on the one-dimensional heat advection and diffusion equations using the phase and amplitude of the diurnal temperature signals obtained from temperature sensors in the surface water and within the sediment (Tonina et al., 2014; Luce et al., 2013). Streambed elevation is quantified by calculating the sediment thickness between paired sensors in the surface water and streambed (Eq. 1-3). As opposed to other techniques that estimate thermal diffusivity from literature values (Constantz, 1998; Lautz, 2012; Swanson et al., 2010), the proposed method quantifies thermal diffusivity from the temperature time series obtained during a period of approximately 12 days, during which time the streambed elevation does not change. Thermal diffusivity is kept constant, and the sediment thickness is calculated (Eq. 3). Bed elevations are calculated by the addition of the sediment thickness to the temperature sensor elevations (DeWeese, 2015):

$$\eta = \frac{-ln(\frac{A_2}{A_1})}{\phi_2 - \phi_1} = \frac{-ln(A_r)}{\Delta\phi} \quad (1)$$

$$Ke = \frac{\omega \Delta z^2}{\Delta\phi^2} * \frac{\eta}{1+\eta^2} \quad (2)$$

$$\Delta z = \Delta\phi\sqrt{\frac{K_e}{\omega}(\eta + \frac{1}{\eta}} \quad (3)$$

where A is the amplitude of the signal, $\boldsymbol{\varphi}$ is the phase of the signal, η is the ratio of the change in amplitude and phase of the paired temperature signals, K_e is the effective thermal diffusivity of the sediment, ω is the conversion from time into radians, and Δz is the calculated sediment thickness above the sensor in the sediment.

Thermal diffusivity is the measure of heat transfer through a medium expressed as area over time. Thermal diffusivity is a component of the diffusion and dispersion of heat through an object, which is affected by the thermal conductivity, the density of the object, specific heat, and velocity through the medium. This method uses the effective thermal diffusivity, which quantifies thermal diffusion, but does not consider the thermal diffusion of the object. In this thesis, the effective thermal diffusivity is referred to as Ke.

1.2.2 Thermal Scour/Deposition Chain Probe

Figure 1.2. A TSDC probe with scour chain

The temperature-based scour monitoring system uses the same design developed in previous work by Tonina et al. (2014) and DeWeese (2015) (**Figure 1.2**). The TSDC probe runs from 1–1.5 meters in length with waterproof temperature sensors spaced 15 cm apart. The probe itself uses a hollow plastic bar. Holes are bored into the plastic bar, spaced every 15 cm, and the sensors are run through the hollowed section to each hole. An aluminum drive tip is fixed on the tip of the probe to facilitate driving it into the streambed. A scour chain is attached to the drive tip to validate the method with maximum scour.

Two different types of data loggers were deployed in this project, a non-telemetry logger and a telemetry logger. The non-telemetry system consists of the following: an Arduino Uno, real-time clock (RTC) shield, SD card, and battery pack. The non-telemetry data logger uses an Arduino Uno as the microcontroller of the data logger that communicates with an RTC and the temperature sensors. Every 15 minutes, the RTC wakes up the system to record the temperature data. The system runs on 6 AA batteries, which provide reliable power for at least nine months.

The telemetry setup consists of a more complex shield and has a more complex system code allowing data to be sent virtually (**Figure 1.3**). The telemetry setup consists of an Arduino mega, GSM cellular shield, RTC shield, SD card, battery pack, and a solar panel for power. The system uses a 2G cellular data line to send temperature data from the site location to a graphical user interface (GUI), ThingSpeak. ThingSpeak is an open-source website used as a graphical user interface (GUI), which uses MATLAB to store data and create visual plots. Temperature data is collected every 15 minutes and stored on the SD card. Using the 2G cellular data line, data is sent every hour for the previous hour of data collection. The telemetry system is powered by a battery pack charged by a voltaic solar panel, which provides power to the data logger throughout the year. In the case that the solar panel does not recharge its battery pack quickly enough, a separate battery back with 6 AA batteries provides power to the system while the solar system recharges.

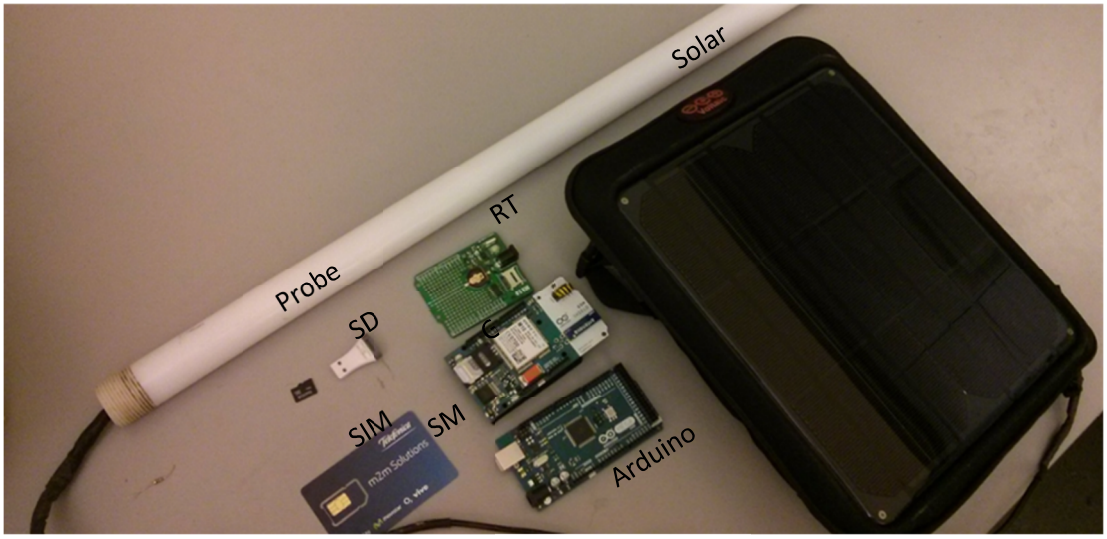

Figure 1.3. TSDC with Telemetry System and its component parts

1.2.3 Project Installation

For this project, the location of the probe is limited to wadable areas and the probability that a local scour event may occur. At the location, a pilot hole is drilled into the streambed using a 3-foot concrete drill bit. The TSDC probe is then placed into a steel pipe and driven vertically into the pilot hole using a combination of a sledgehammer and a fence post hammer. The probe is driven into the streambed to a depth that leaves at least one sensor in the surface water. After the probe is securely in the streambed, the steel pipe is removed, leaving the instrument in the substrate. A 20–30 ft cable is run through half-inch, non-metallic flexible conduit to protect the wires. The conduit is fastened to the side of the bridge pier using concrete anchors and half-inch steel straps. The data logger is placed inside a Pelican case and strapped beneath the bridge deck or any other place where it is out of reach and sight of the public to prevent vandalism. The cable wires are then run up to the data logger and connected to the Arduino micro-controller using a waterproof cable set. The system is run either by a 6 AA battery pack or by a solar panel that is connected to the data logger.

Except for the control bridge, each site had two probes. Once the probes were installed, a survey was taken using an engineering auto level and stadia rod. Three measurements were taken at the streambed, at the top of the probe, and at a landmark that does not move. An example of a landmark that was used at most bridge sites was one of the conduit anchors on the bridge pier. The

streambed and top of probe measurements were compared with the elevation of the landmark to determine the change in bed elevation as well as to determine if the probe itself had shifted.

1.2.4 Data Analysis and Verification

Each temperature sensor buried in the sediment is paired with a sensor in the surface water in order to quantify the amplitude ratio and phase shift between surface and subsurface water temperatures (Tonina et al., 2014). The amplitude and phase of each signal was computed using the Discrete Fourier Transforms (Luce et al., 2013) with a two-day window. All method programming was done in the R programming language using RStudio, an open source language program. Once the amplitude and phase of each signal was quantified, Equations 1, 2, and 3 were used to determine the thickness of the sediment above each temperature sensor in the sediment.

Addition of the calculated sediment thickness and sensor elevation, obtained from the original survey, results in the new bed elevation. When a scour or deposition event occurs that covers or reveals a sensor to the surface water, the method switched the analyzed sensor to compare the first sensor in the sediment with the surface water sensor. This method was able to continuously analyze data over time.

A maximum scour chain and monthly streambed elevation surveys using the three original measurements taken at installation were the two methods utilized to verify results from the Discrete Fourier Transform. While each probe was fixed with a scour chain, the bridge in Pine, ID was also paired with monthly surveyed bed elevations. The Banks, Pinehurst, and Salmon Bridges were verified using a maximum scour chain, but not with monthly surveys due to the travel time to the sites and consistently high flows. The number of chain links out of the bed was counted upon installation and on the last site visit. When a scour event occurred, the flow from the river pushed the chain that is not lodged in sediment in the downstream direction. On the last site visit, the first chain link to be found vertical in the sediment is deemed the location of maximum scour. Using the difference between the number of links upon installation and on the last data collection date along with the length of each chain segment, the maximum scour is computed.

Pine Bridge was verified with monthly elevation surveys, but high flows prevented an accurate measurement of the scour chain. Each survey consisted of the same three measurements described previously. Comparing the measurements upon installation and at each survey point provided continuous verification of streambed elevation.

Camas Creek Bridge was not verified with either method because of the hardship with data collection at this site; the data signal at the bridge was very weak, and data was sent only periodically. This site was used to test the telemetry system that used a Wi-Fi chip to communicate between two different Arduino micro-controllers. One data-logger was installed at the bridge; the second was elevated on a power line pole in an effort to receive a stronger signal. The bridge data logger sent the data to the logger with the GSM cellular shield every four hours. The GSM shield system connected to the data network and sent the collected data to ThingSpeak; however, the signal was only strong enough to send data for approximately a week.

1.3 Results

Both the scour chain and calculated bed elevation indicated that the maximum scour was zero at the Banks site (Figure 5); however, the TSDC probe tracked a deposition event of approximately two inches that occurred during low flow events from Fall 2015 to February 2016. This deposition event was then scoured to the original bed elevation during higher flow events. This pattern of deposition and scour appears to occur on a yearly basis. A noise level of approximately ±2.5 cm is present throughout the year. From the middle of November 2015 to late Fall 2016, no data were collected due to persistent ice formed around the probe causing impedance of an oscillating signal into the sediment.

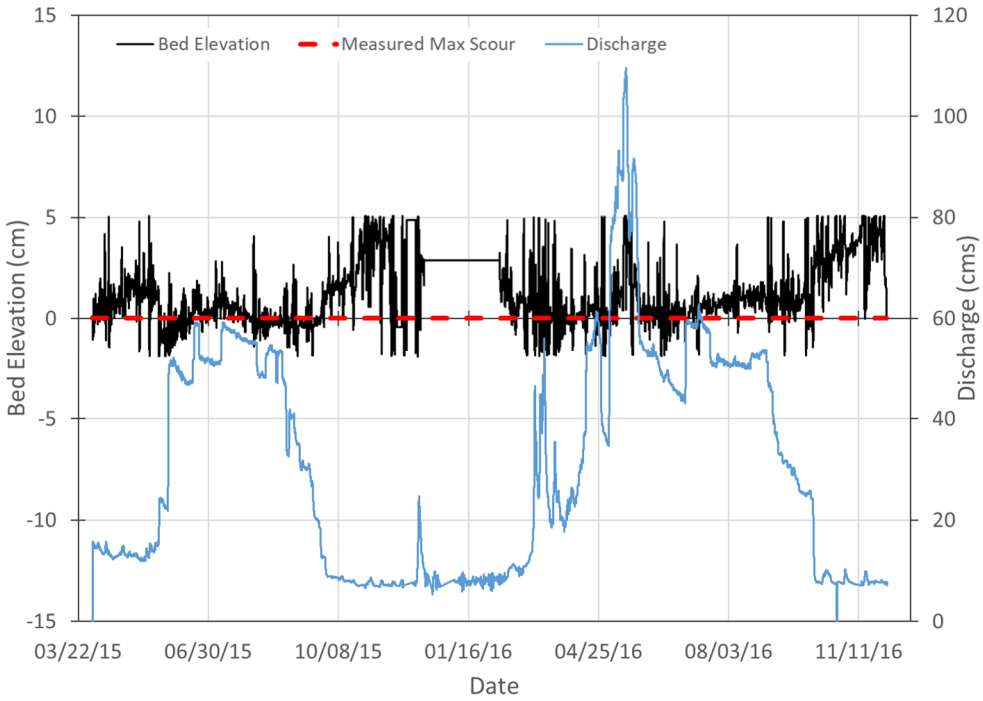

Figure 1.4. Calculated bed elevation and measured maximum scour at Banks Bridge

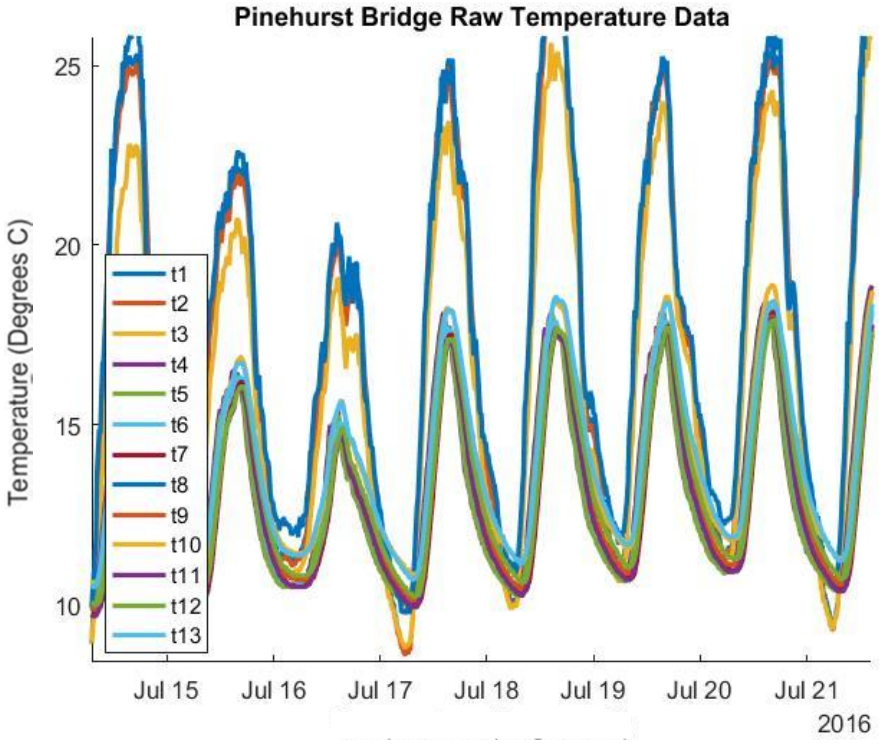

Figure 1.5. Raw temperature data collected at Pinehurst Bridge

The probes at Pinehurst Bridge had a sensor malfunction and no data could be extracted from the signal. Many of the raw temperature signals extracted from the data lay on top of one another, so the sensors could not be differentiated (**Figure 1.5**). This overlapping of signals created the same phase or no lag in the time between signals, which correlated to every sensor located either in the water or in the sediment. Because of its remote location, Pinehurst Bridge was visited only twice during the study period.

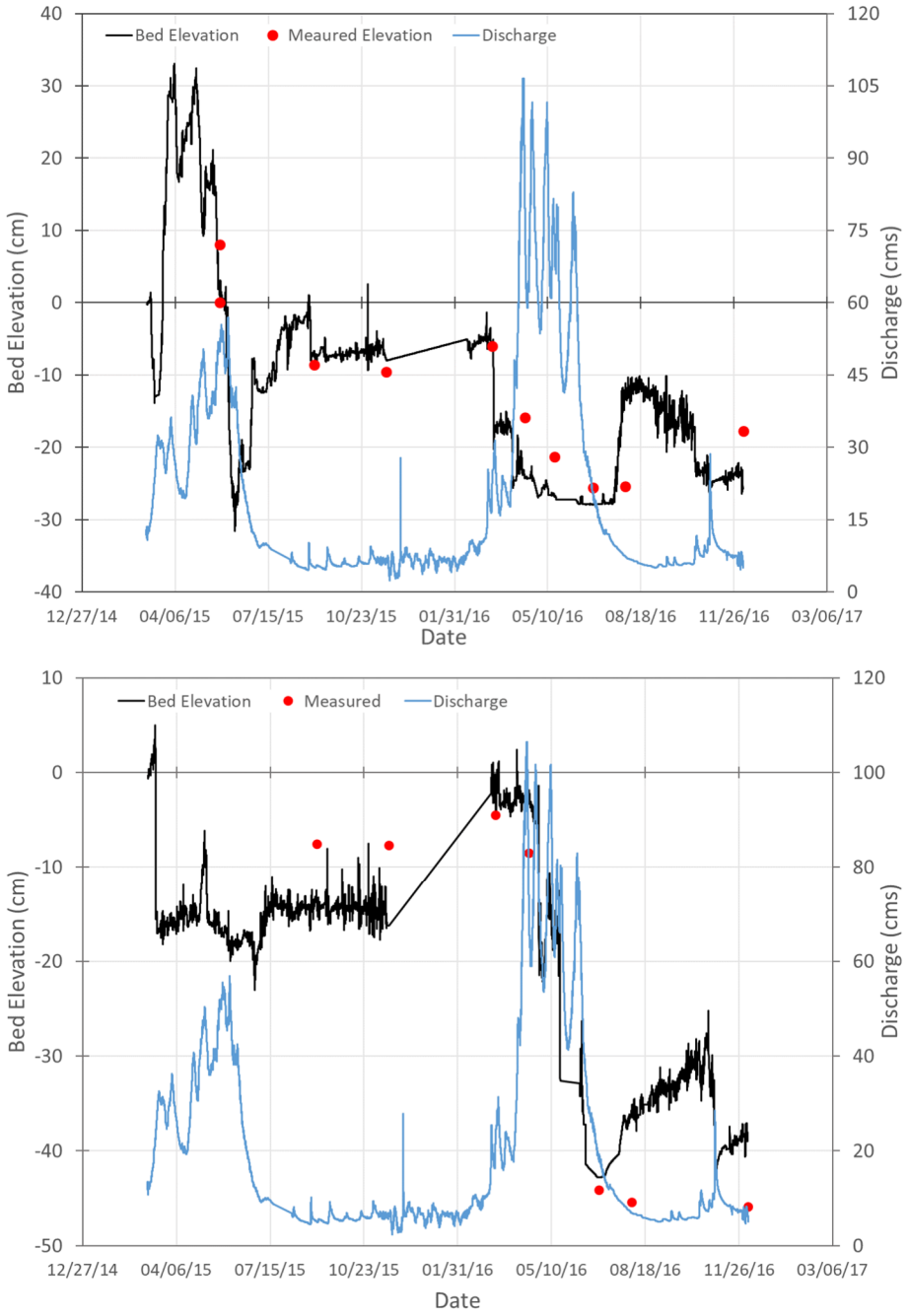

Figure 1.6 - Calculated vs. measured bed elevations at Pine Bridge. Top panel is Probe 1; Bottom panel is Probe 2.

The TSDC predicted bed elevations closely matched those surveyed at both probe locations (**Figure 1.6**). The maximum scour from the scour chain was not available, because the water level at the time of data collection was too high to reach the scour chain. During the final data collections, neither TSDC probe was longer lodged in the sediment. There was no scour event that would have exceeded the depth of the probes; however, debris buildup on the bridge was observed. It is probable that debris carried downstream dislodged the sediment probes.

The downstream probe has an average error of approximately 10 cm; however, the calculated bed elevations followed same trends as the surveyed elevations. Continuous monitoring indicated an annual scour/deposition pattern. A scour event occurs in the Spring, followed by a constant bed elevation to the winter months when deposition occurs. The maximum scour calculated at the downstream probe was 46 cm. The upstream probe had a high level of accuracy in the first half of the data collection period, with an error of less than 2.5 cm, but with performance less accurate from March 2016 to December 2016. Like the downstream probe, a scour event occurred in the spring, but with a deposition event occurring soon after. Another rapid scour and then deposition event occurred from July 2015 to August 2015. During the fall and winter months, the bed elevation remained roughly constant, followed by another scour and deposition event similar to the previous year. Throughout the monitoring period, the maximum scour of Probe 1 was 35 cm.

TSDC performance had high precision at the Lemhi Bridge (Figure 1.7). Probe L1 had a maximum scour chain measurement of 10 cm and a calculated maximum scour at just over 10 cm. Probe L2 measured a maximum scour of approximately 20.3 cm, and a calculated maximum scour of 25.4 cm. Both probes exhibited a similar pattern of scour early in data collection followed by deposition in the summer. The calculated bed elevation varied approximately 5 cm from the maximum scour chain measurement at Lemhi Bridge.

As discussed previously, the Camas Creek Bridge had issues with the telemetry system, but some data were collected from Probe C1 (**Figure 1.8**). Data were not sent to ThingSpeak from April 2016 to June 2016; however, data were collected and sent to ThingSpeak from the middle of March 2016 to April 2016 and again in June 2016. During times of data collection, bed elevation remained roughly constant, except in the middle of June when 12.7 cm of deposition occurred.

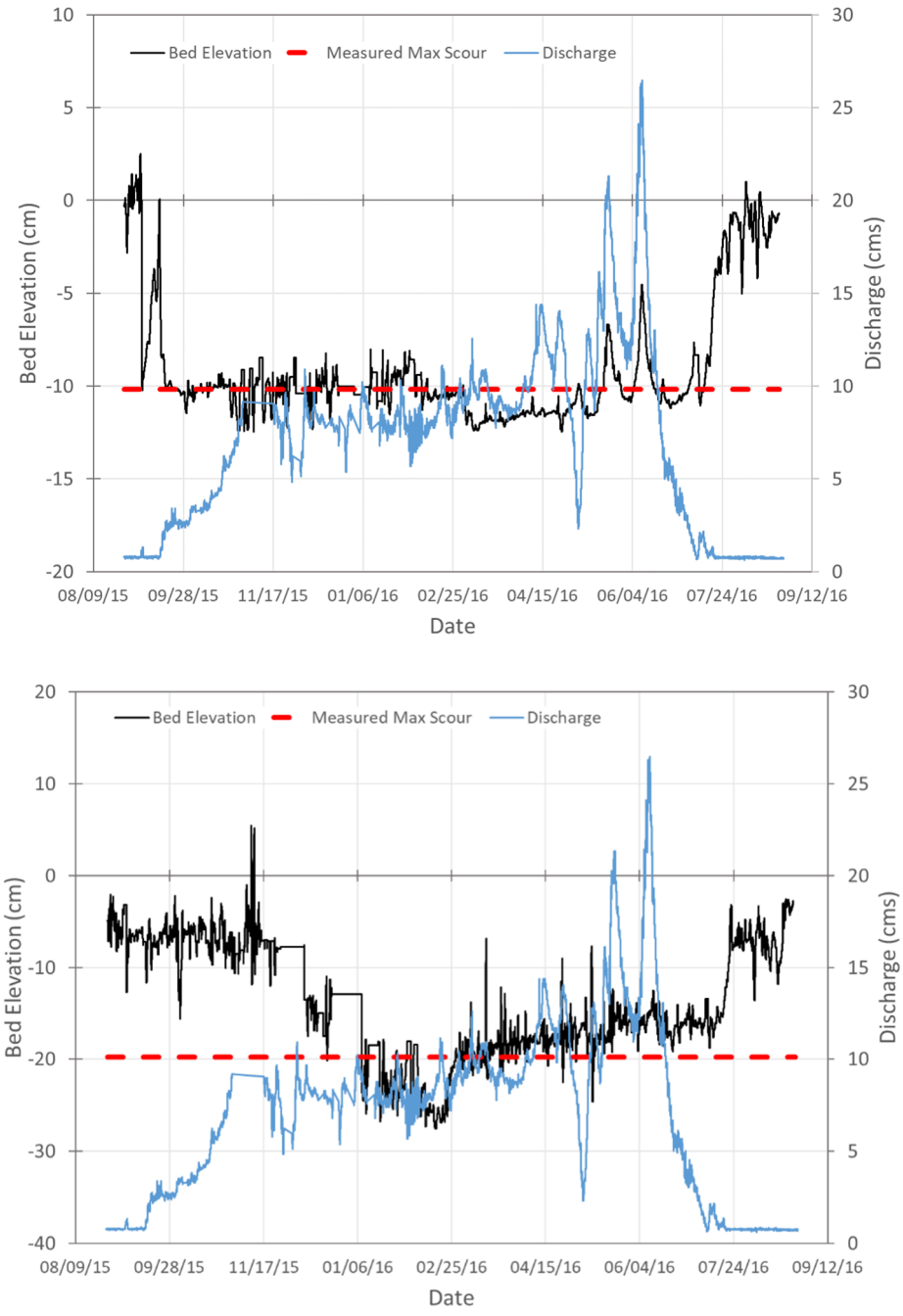

Figure 1.7. Calculated vs. measured bed elevation at Lemhi Bridge. Top panel is Probe L1; bottom panel is Probe L2.

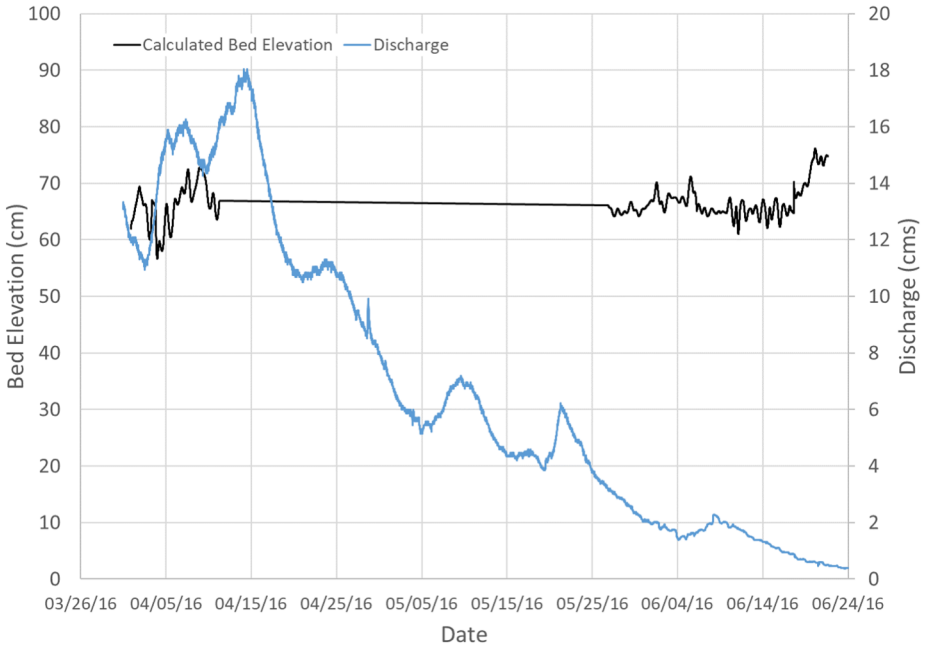

Figure 1.8. Bed Elevation calculated at Camas Bridge (Probe C1).

A high-water year in 2017 made it difficult to successfully collect data and survey the Camas and Pine Bridges. Flooding and high water created obstructions to roadways and did not allow access to the water (Figure 10). Due to high water levels, I expected to see a great deal of scour at some bridge sites. At the Pine Bridge, the TSDC probes were no longer in the streambed by the end of data collection.

Figure 1.9. Camas Bridge in May 2017.

1.4 Conclusions and Recommendations

Comparison of both maximum scour and time series show agreement between TSDC and ground surveyed stream elevations. The maximum error was ten (10) cm, when compared to the surveyed stream elevation, and occurred at the end of the data collection period at Pine Bridge. I hypothesized that this error is the result of the change in sediment composition, from fine sand to coarse gravel (Figure 7). Pine Bridge has a gravel bar migrating downstream below the bridge, depositing a different substrate at the probe location from that observed during installation. During installation, the substrate consisted of fine sand and silt material, while the substrate consisted of gravels and cobbles at the last ground survey. The change in substrate may cause a potential limitation to the method because thermal properties may change with substrate size. However, I do not know the sensitivity of the error due to changes from sand to coarse gravel. Additional research is needed to quantify the effect of changes in sediment type on thermal properties. To account for the change in substrate in the method, the Ke of the sediment must be recalculated for a period during which there is no change in bed elevation, and then held constant for the rest of the data collection period. As it relates to bridge scour, feet of erosion are of more interest than a few inches. At sites where the substrate did not change (Banks and Pine Bridges), the measured maximum scour using the scour chain correlated closely with the calculated values.

Some uncertainty about the size of the grain material also arises from the measurement of the streambed. The streambed is a rough surface with variable elevation depending on where a survey measurement is placed on the streambed. For example, during a survey, the top of a grain may be measured, while the method is measuring from the bottom of the grain or the mid-point of the grain size. Therefore, some uncertainty is due to survey measurements of a rough surface, such as at the Pine Bridge site.

The maximum scour chain value was not obtained at the Pine Bridge site, because the scour chain data was not available. On the last data collection visit, the probes were no longer in the streambed even though data analysis does not indicate there was a scour event large enough to scour below the depth of the probes. A large amount of debris was wrapped around the bridge pier. It is believed that the debris passing by the bridge pier entangled with the temperature probe wires and ripped the temperature probes out of the streambed. Moreover, the Camas Bridge site was not accessible for the last data collection date due to the washout of the roadway, and the scour chain data was not able to be collected.

The results of this method of determining bed elevation captured a very dynamic system with multiple scour and deposition events that would otherwise not have been tracked with annual or biannual surveys. Yearly measurements may provide a false picture of stationary streambed elevation, when both scour and deposition events are occurring (Prendergast et al., 2014). The Banks and Salmon Bridges experienced a pattern of scour followed by deposition up to the original bed elevation at low flows. This pattern seems to occur yearly, which also may not be captured by annual surveys of the bridge pier. While a yearly survey may detect the scour event, it will miss the deposition event. The assumption that the same amount of scour occurs each year which may result in overdesigning scour prevention techniques.

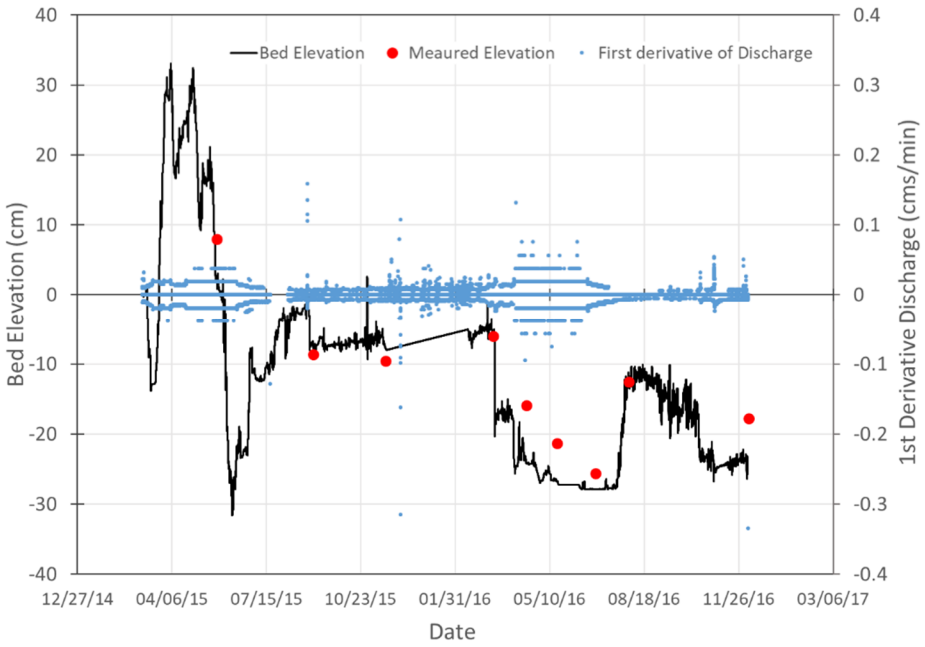

Figure 1.10. Bed elevation (Probe 1) and daily rate of change of water flow at Pine Bridge.

Scour events are often said to be correlated with flood or high flow events (Fisher and Khan, 2013; Topczewski et al., 2016; Zarafshan et al., 2012; Tao et al., 2013); however, the results suggest that high flow is not the only cause of scour events. High discharge and scour had little correlation at all of the bridge sites in this study. I hypothesize that local conditions, such as sediment supply, have more to do with the amount of scour than high flows. The results also reveal a correlation between scour and the rate of change in discharge (**Figure 1.10**). When a rapid increase in discharge occurs at our bridge location, a scour event happens. I believe that these rapid changes may cause a larger scour because of the change in flow characteristics at the bridge. Rapid changes of slow to fast velocities around the pier cause rapid change in shear stress allowing particles to move. The results

also revealed that in some instances when the discharge is at the highest of the year, the maximum scour has already occurred. The results suggest that multiple events contribute to the occurrence of scour rather than just high flow events.

Pinehurst Bridge was the only site where there was difficulty analyzing the temperature data to obtain a bed elevation. The phase or lag of the signal propagating through the sediment was inconsistent. Phenomena such as upwelling, stratified sediment composition, large material, and data location are all factors that could have influenced the calculation of bed elevation at this site and caused distortion of the signal. Also, the probe sensors may have malfunctioned or not been correct, resulting in several temperature sensors having nearly identical signals.

The results for testing the telemetry system at Camas Creek Bridge show that reliable coverage is necessary. There were times when the temperature data was reliably sent to ThingSpeak; at other times, the system stopped working, came back online, but then shut down again. I suggest that this was due to the instability of the service connection at the bridge location, which was verified after talking to local residents who acknowledged the lack of reliable cellular service in the area. I was able to set up a system in the city of Boise, in which temperature data is continuously sent to ThingSpeak every hour. The same 2G cellular service as that at Camas Creek Bridge was used reliably over several months. The telemetry system is a viable system for transmitting temperature data but requires more reliable cell service.

Based on the findings of this study, this report provides the following recommendations to improve this method:

- Research the effects of different substrate composition on thermal properties of the sediment.
- Determine a method to analyze the thermal property in real-time without requiring the bed elevation to remain constant. This will increase the accuracy of this method by eliminating the assumption that thermal properties are constant.
- Reduce the error in the method by utilizing a different data processing method that limits the effects of sudden temperature changes. This will provide for more accurate representation of stream bed elevations.

- Develop a new temperature sensor probe that is thinner and has no exposed wires. Developing a thinner probe with no exposed wires will allow the method to be deployed in a wider range of areas and application. A thinner probe will allow for easier installation into the streambed.

The method presented in this chapter provides an accurate way to measure scour and deposition processes to help in bridge design and to assess the stability of bridges. I was able to verify the method in the field by using a combination of a scour chain and periodic field surveys. In this study, I was able to continuously collect data at the majority of the sites for over a year, tracking the streambed elevation within a couple of cm of the actual bed elevation. Although, processing the data still requires manual input, with a few adjustments to the coding the method can be used to monitor streambed elevations in real-time. The coding can be adjusted to detect scour every fifteen minutes by comparing the temperature signals, and a warning system can be implemented. Despite, the few flaws in the data logging system, the method proved to be a reliable in continuously monitoring streambed changes and scour with a minimum amount of manual labor. The temperature-based method is not limited to bridge scour monitoring but can be extended to other monitoring and research applications. Using an array of temperature probes placed perpendicularly to the flow, this method can be used to determine water depths and streambed elevations along a cross section. By adding multiple cross sections of temperature probes along the river, the evolution of the morphology of the river can be followed. A research extension of this method includes using the temperature-based systems to determine the number of fines in the streambed. As this report demonstrates, using a temperature-based method is an easily deployable monitoring system for determining streambed elevations and can be extended into further applications within streambed morphology.

Chapter 2. USING DIURNAL TEMPERATURE SIGNALS TO DETERMINE THERMAL PROPERTIES OF SEDIMENT AND HOW IT RELATES TO POROSITY

2.1 Introduction

Anthropogenic disturbances near streams are known to have many effects on ecosystems from chemical to physical. Some of these disturbances may cause increases in the amount of fine sediment influx into river systems. New construction of roads, trails, urbanization, and other developments besides tree harvesting may release fine sediment into rivers.

The introduction of large amounts of fine sediment into rivers results in filling of voids among coarse grains, a process called clogging, which leads to reduced interstitial velocities (Cui et. al., 2008). The reduction of interstitial flows may also reduce the water exchange between stream and its streambed, which forms a near surface band of sediment, referred as hyporheic zone, mainly saturated with stream water. The hyporheic zone hosts many organisms which dwell permanently or during a stage of their life (Rabeni et. al., 2005; Nogaro et. al., 2010). For example, fish, such as salmon, lay their eggs within the hyporheic zone of a gravel-bed (Platts et. al, 1979). Coarse gravel allows enough hyporheic flow to transport oxygen-rich surface water to and remove waste product from fish embryos (Greig et. al., 2005), whereas clogging of gravel may impair embryos habitat by reducing this flow. It is becoming increasingly important to quantify and monitor the amount of fine infiltration as anthropogenic activities, such as roads, urbanization and water diversion, are introducing more fines into waterways than without human impacts.

As fine sediment infiltrates and clogs, the streambed thermal properties and porosity change (Tonina et. al, 2014). A relation between sediment thermal properties and porosity may help quantifying the amount of fine sediment within streambed substrate. Several investigations have been conducted to quantify the amount of sediment infiltration into the streambed. In Einstein (1968) performed an experiment in a laboratory flume that demonstrated how fine sediment would fill the voids of the larger material by settling at the bottom first. It was later determined that sediment would infiltrate to a depth that was within a few diameters of the largest bed material (Schälchi 1992). A method that used hydraulic conductivity to evaluate streambed clogging found a lack of relationships between surface grain size and streambed hydraulic conductivity at the reach-scale (Datry et. al., 2015).

Tonina et al. (2014) and Luce et al. (2013) proposed a method, which analyzes the change in diurnal temperature signal between the stream and pore waters to quantify thermal properties of sediment. The method also estimates changes in streambed elevation and hyporheic fluxes; however, estimation of streambed elevation and hyporheic fluxes depends on sediment composition, which changes as fines clog porous material. The method evaluates the thermal property of the sediment during a period when the streambed elevation is known and constant. Once the thermal property is known, it is selected and kept constant, allowing streambed elevations to vary. Sediment load from upstream and deposition may change the sediment composition leading to inaccuracies in the estimated stream bed elevations. If the composition of the streambed remains the same after scour and deposition the thermal properties will remain the same. A study of the relationship between sediment thermal property and composition will help constrain the variability of the thermal property as a function of sediment rather than streambed elevation.

Determining a way to quantify the thermal property of the sediment and relate it to sediment composition can give insight in river morphology, streambed clogging, and sediment composition without having to physically be on-site. This study focuses on analyzing the variability of the thermal property of the streambed substrate as fines are added to a gravel matrix and hypothesize that changes in thermal properties could be used to determine sediment clogging.

2.2 Method

2.2.1 Theory

This method uses the same one-dimensional heat advection and diffusion equations from the work of Tonina et al. (2014). The amplitude and phase of a temperature signal propagating through the sediment provide information on how quickly heat is dispersing as it travels through the sediment (Tonina et al., 2014; DeWeese, 2015). As the streambed clogs with fine sediment, the composition changes and so its porosity causing its thermal property (Ke) to change. This project uses the equation proposed by Luce et al. (2013) to monitor the Ke profile for different sediment composition and during a simulated streambed clogging:

$$Ke = \frac{\omega \Delta z^2}{\Delta \phi^2} * \frac{\eta}{1+\eta^2} \quad (1)$$

Sediment infiltration is greatly dependent on the size ratio between the gravel and fine sediment (Jackson, 1979, Frostick et al., 1984). The sediment composition switches from frame-supported (gravel) to matrix-supported (sand) when the fine sediment fraction within the pores of the gravel matrix equals that of the saturated fine sediment fraction (Wooster et al., 2008). In the frame-supported sediment composition the gravel particles are touching, while the matrix-supported composition, the fine sediment is filling the voids of the gravel particles so that they are not touching. Equation 2 (Wooster et. al., 2008) was developed using the porosity, particle size, and standard deviation of sediment composition distribution to estimate the saturated fine sediment fraction for a specific composition (Wooster et al., 2008).

$$f_s = \frac{0.621(1-0.621\sigma_{sg}^{-0.659})\sigma_{gg}^{-0.659}}{1-0.621^2(\sigma_{gg}\sigma_{sg})^{-0.659}} f_n\left(\frac{D_g}{D_s}\right) \quad (2)$$

where f_s is the saturated fine sediment fraction, σ_{sg} is the standard deviation of the sand, σ_{gg} is the standard deviation of the pea pebble, D_s is the geometric mean of the sand, and D_g is the geometric mean of the pea pebble. Geometric mean and standard deviation were calculated from the sediment gradation curves. Equation (2) was used to quantify the amount of sand to add to the gravel in the laboratory experiments from clean gravel to fully sand saturated gravel. We studied 4 cases at 25, 50, 75 and 100% of gravel pore saturation by sand. The calculated fine sediment fraction can be found in Appendix A.

2.2.2 Lab Experiment

A laboratory experiment was conducted to test the hypothesis, which used a diurnal temperature signal to track sediment composition changes. The laboratory experiment consisted of a sediment tank that was fed with water from two reservoirs, one hot and one cold (Figure 12). A PID controlled mixing valve mixed an amount of cold water and hot water before entering the sediment tank creating a sinusoidal curve with a 2-hour period, which mimicked daily stream water temperature fluctuations. A 2-hour period was chosen to allow for more cycles to be collected in a shorter amount of time during the test.

The vertical velocity through the tank was controlled by using the total head in the tank and a standpipe to drain any excess flow. A tube located at the bottom of the tank created a vertical downwelling velocity. A tipping bucket and the surface area of the tank tracked the downwelling velocity through the sediment. The velocity throughout the experiment was designed to average

approximately 0.0018 cm/s. The total head was adjusted between experiments, to introduce the same velocity through the sediment, by raising and lowering the outlet tube.

A thermal scour probe, similar to the one described in chapter one, measured temperature data over time. The probe was centered in the sediment tank to avoid disruption of the temperature signal caused by the sides of the tank. Temperature sensors were spaced out every five centimeters to increase resolution of the system. The temperature sensors were controlled by a micro-controller to collect data every minute. Collecting data every minute allowed for a better represented temperature signal. The spacing between the sensors and data collection frequency allowed for the ability to detect significant features, such as the peaks, in the signal to calculate the Ke of the sediment.

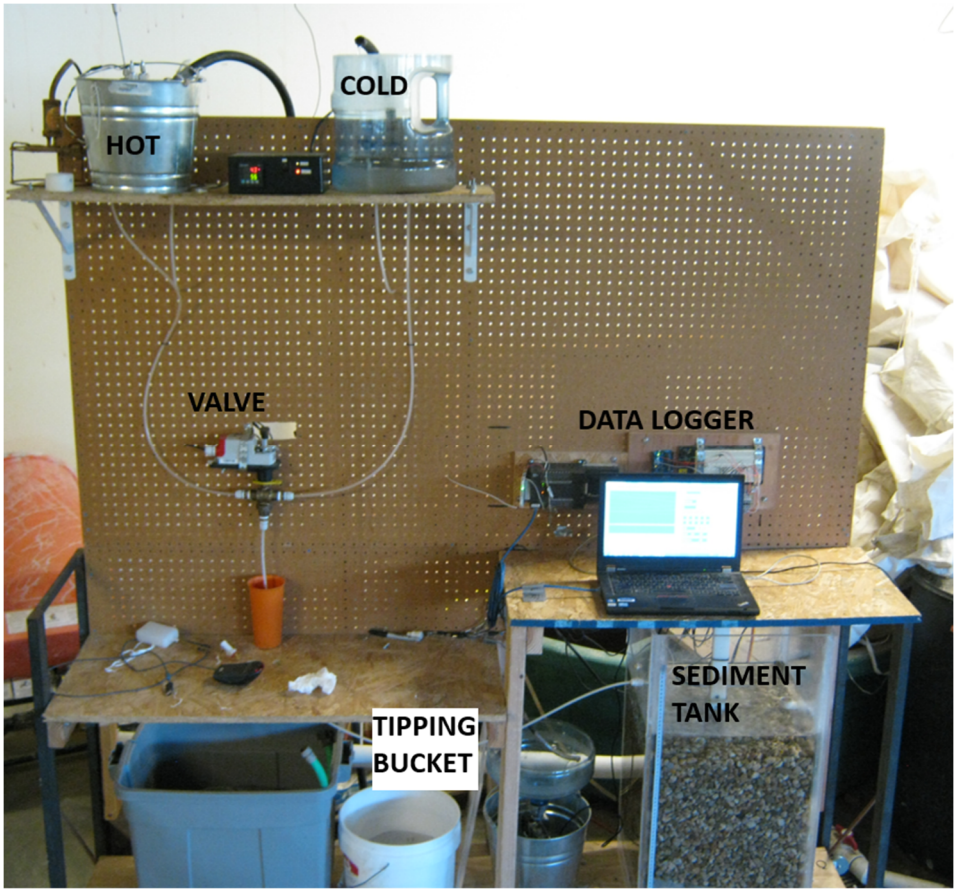

Figure 2.1 – Photograph of the sediment tank laboratory setup used in the experiments.

Eight total experiments were conducted to relate thermal properties and sediment composition. The experiments consisted of the following compositions: river rock (RR) with a d_{50} of 15.5 mm, pea pebble with a d_{50} of 4.1 mm, four experiments with varying amounts of sand added to

the pea pebble mixture (pea pebble-sand saturation experiments 25% to 100%), well sorted sand with a d_{50} of 0.3 mm, and a river rock with sand infiltration test (Table 2.1).

Table 2.1 – Table of measured porosity and median grain size of soils used in experiments.

	River Rock	Pea Pebble	Pea Pebble with 25% Sand Saturation	Pea Pebble with 50% Sand Saturation	Pea Pebble with 75% Sand Saturation	Pea Pebble with 100% Sand Saturation	Sand
Porosity (measured)	0.460	0.450	0.470	0.460	0.430	0.450	0.360
Porosity (Calculated Equation 3)	0.374	0.498	0.491	0.486	0.482	0.477	0.210
D_{50} (mm)	15.5	4.18	4.16	4.15	4.12	4.10	0.300

The river rock and sand were obtained from the University of Idaho Center for Ecohydraulics lab and the pea pebbles were obtained from Home Depot. Each sediment type was thoroughly cleaned to remove fine material. Each sediment composition was placed into the tank and leveled to a constant surface elevation. To limit the amount of air that could remain trapped in sediment voids, the tank was slowly filled. A temperature signal travels differently through air than water, causing an error in the Ke calculation if air bubbles were present. The sediment was allowed to settle for 12–24 hours before data collection began. As the sediment settles, the thermal properties could change as voids within the sediment shift and are filled by smaller particles.

The river rock test was conducted by placing the sediment into the tank and leveling the surface. Temperature data was collected for several days. Once the data collection was deemed successful, the river rock was removed from the tank and placed aside. The pea pebble composition was then placed into the tank using the same process.

The pea pebble tests with an added amount of sand (25%, 50%, 75%, and 100% sand saturation of its pores) experiments were mixed using a concrete mixer. Using the concrete mixer, the pea pebble and sand were mixed for half an hour to an hour to allow for a more uniform mix of the sediment composition. Some water was added to the mixer to allow the sediments to mix without the sand settling out. Once each pea pebble with fine sediment mixture lab experiment was completed, it was placed back into the mixer, and an additional amount of sand was added for the

next experiment. This process was continued until the last pea pebble with sand experiment was completed.

Sand was added to the pea pebble mixture in increments of two pounds or 0.91 kilograms. Therefore, the pea pebble sand-mixture Experiment 1 added 0.91 kilograms (25% saturation), Experiment 2 added 1.82 kilograms (50% saturation), Experiment 3 added 2.73 kilograms (75% saturation), and Experiment 4 added 3.64 kilograms (100% saturation) of sand. The sand fraction for Experiments 1 – 4 were 1.1, 2.1, 3.2 and 4.2 % by weight, respectively. Calculations for the sand fraction can be found in Appendix A. Each pea pebble-sand mixture experiment was conducted for a minimum of two days in order to allow the sediment to settle and collect an appropriate amount of data.

Once the pea pebble tests were completed, the sediment tank was filled with well sorted clean sand. The surface of the sand was evened, and the elevation of the bed was measured to calculate Ke. This test was conducted for a minimum of 2 days to allow the sand to settle and the Ke to be consistent.

The last experiment was completed by alternating layers of river rock and clean sand approximately every 15 cm, with a sand layer on top, to determine how sediment infiltration affects Ke. The sediment layer thickness was chosen so that multiple temperature sensors would be in each layer. The fine sediment (sand) was allowed to fall into the interstitial pores of the river rock without any bed disturbances. This experiment is designed to imitate a natural occurrence of fine sediment infiltration that may occur in many gravel-bed streams and rivers.

2.2.3 Data Analysis and Verification.

Each temperature sensor in the sediment is paired with the sensor in the water to determine the change in amplitude and phase of the temperature signal as it passes through the sediment (Tonina et. al. 2014) with a two-day window Discrete Fourier Transform (Luce et. al. 2011). The Discrete Fourier Transform was written in RStudio, an open source language. Other methods, such as, VFlux (Gordan et. al. 2012), 1DTempPro (Voyteck et. al., 2013) and others (Lautz, 2012; Rau et. al., 2014) are also available to analyze the amplitude and phase.

Equation 1 quantifies the Ke and its relationship with sediment composition. After each test, the calculated velocity, phase, and amplitude were compared at different depths. Comparing these

variables at different depths allowed the location of the temperature signal that could most accurately represent Ke.

Porosity is a measure of the amount of empty space in a sample of sediment. Sediment porosity was determined by taking the volume of voids, subtracting the volume of solids, and then dividing by the total volume. This measured porosity was compared with calculated porosity using the following equation by Wooster et. al. (2008):

$$\lambda = 0.621\sigma^{-0.659} \quad (3)$$

where λ is the porosity and σ is the geometric standard deviation derived from the sediment distribution of the sample.

2.3 Results

2.3.1 River Rock

The River Rock had the highest Ke with an average of 0.046 cm^2/s. The Ke varied between each sensor with a minimum of 0.006 cm^2/s and a maximum of 0.085 cm^2/s (**Figure 2.2**). The minimum and maximum thermal diffusivities occurred at sensor 2, approximately 3.9 cm below the sediment-water interface, and sensor 5, approximately 18.9 cm below the sediment-water interface, respectively. The Ke value was the lowest near the surface of the sediment column, increased towards the midpoint of the sediment column, and then decreased again as depth increased past the midpoint. The porosity was measured to be 0.46 and quantified with Wooster et al.'s equation (2008) to be 0.374.

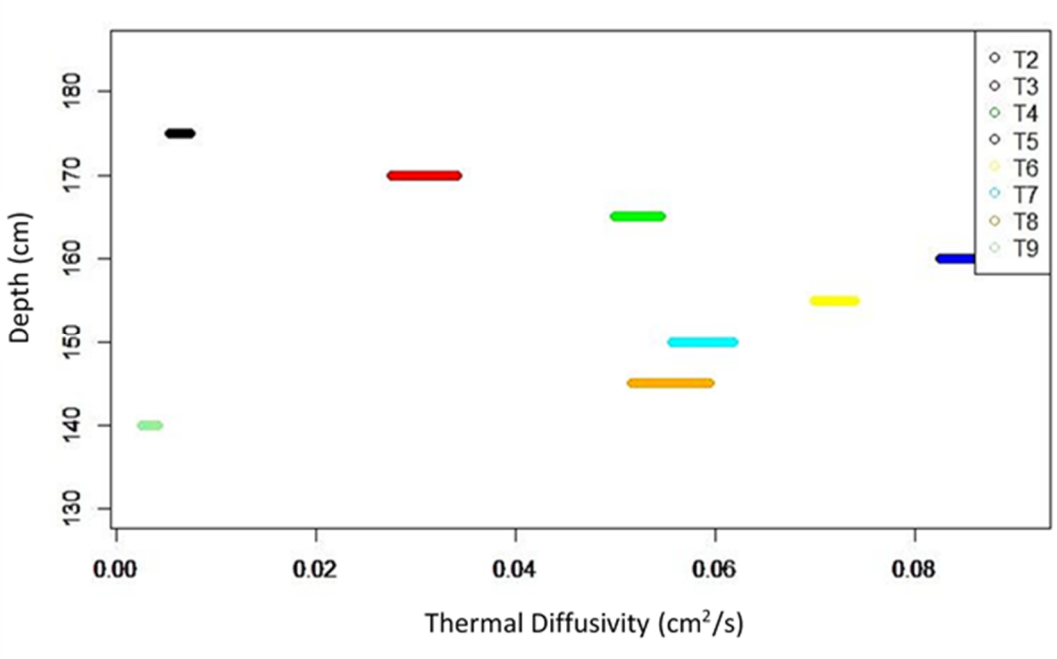

Figure 2.2 Vertical profile of calculated Ke values within the sediment column for the river rock experiment.

2.3.2 Pea Pebble

The Pea Pebble had the second highest thermal diffusivity with an average of 0.0058 cm^2/s. The thermal diffusivity varied between each sensor with a minimum of 0.0013 cm^2/s and a maximum of 0.016 cm^2/s. The maximum and minimum thermal diffusivities occurred at sensor 9, approximately 38.5 cm below the sediment-water interface, and sensor 2, approximately 3.5 cm below the sediment-water interface, respectively. The Ke value was the lowest near the surface of the sediment column, increased towards the midpoint of the sediment column, and then decreased again as depth increased past the midpoint. The measured porosity was 0.45 and that quantified with Wooster et. al. ’s equation (2008) was 0.498.

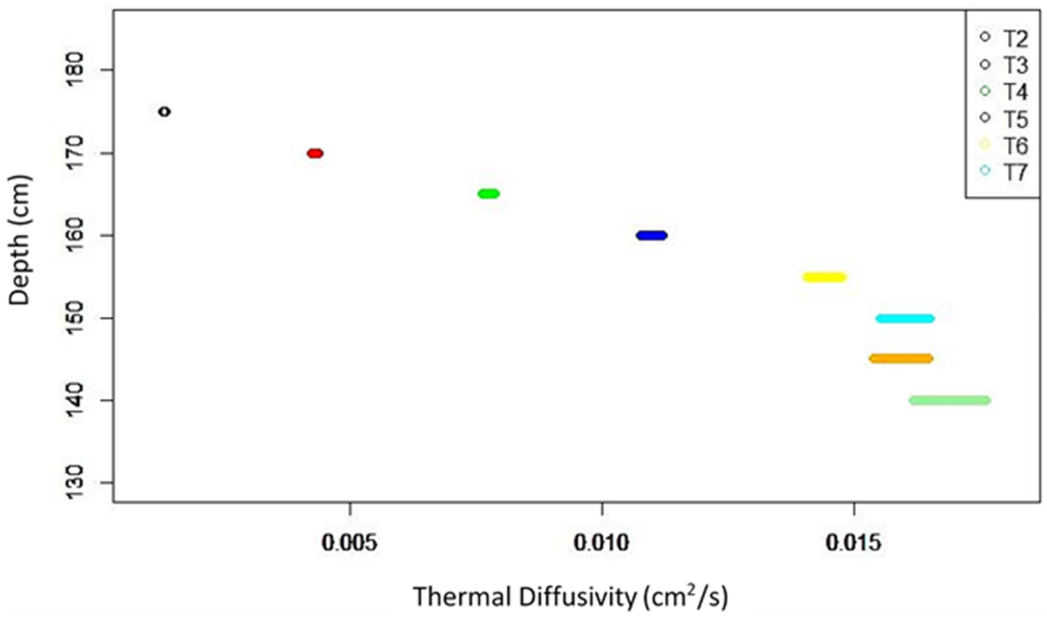

Figure 2.3 – Vertical profile of calculated Ke values within the sediment column for the pure pea pebble experiment.

2.3.3 Pea Pebble with 25% Saturation

The Pea Pebble with 1.1 percent sand fraction had an average thermal diffusivity of 0.0084 cm^2/s. The thermal diffusivity varied between each sensor with a minimum of 0.00082 cm^2/s and a maximum of 0.015 cm^2/s. The maximum and minimum thermal diffusivities occurred at sensor 8, approximately 33.5 cm below the sediment-water interface, and sensor 2, approximately 3.5 cm from the top of the sediment column, respectively. The thermal diffusivity was lowest near the sediment-water interface, increased as it neared the midpoint of the sediment column, and became constant near the bottom of the tank. The measured porosity was 0.47 and that calculated with Wooster et. al.'s equation (2008) was 0.491.

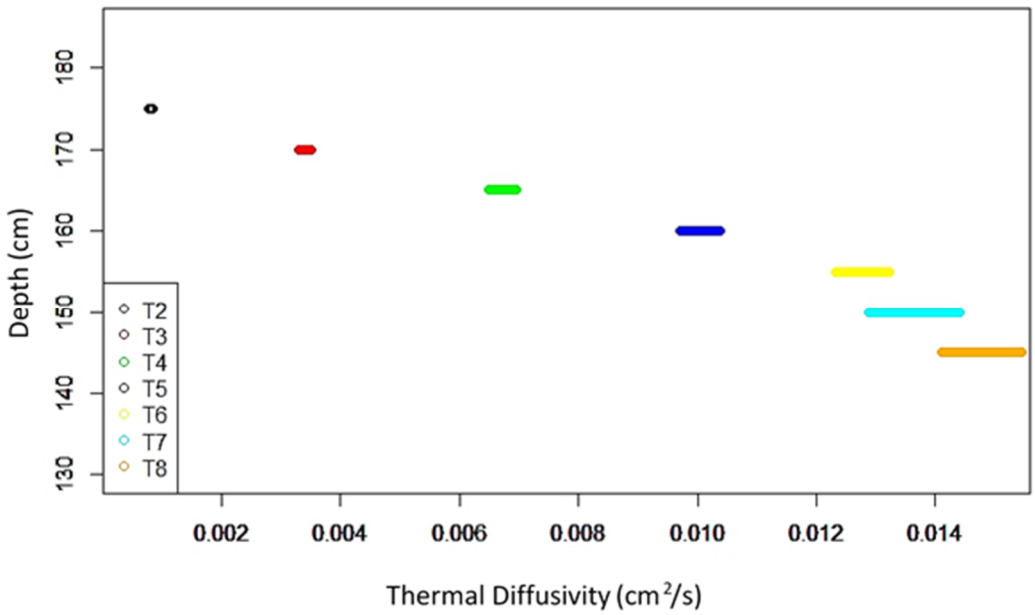

Figure 2.4 – Vertical profile of calculated Ke values within the sediment column for the pea pebble with 25% sand saturation experiment.

2.3.4 Pea Pebble with 50% Sand Saturation

The Pea Pebble with 2.1 percent sand fraction had an average thermal diffusivity of 0.012 cm^2/s. The Ke varied between each sensor with a minimum of 0.0012 cm^2/s and a maximum of 0.018 cm^2/s. The maximum and minimum thermal diffusivities occurred at sensor 9, approximately 38.5 cm from the top of the sediment column, and sensor 2, approximately 3.5 cm from the top of the sediment column, respectively. The Ke value was the lowest near the sediment-water interface and tended to get larger deeper into the sediment column. The measured porosity was 0.46 and that calculated with Wooster et. al.'s equation (2008) was 0.486.

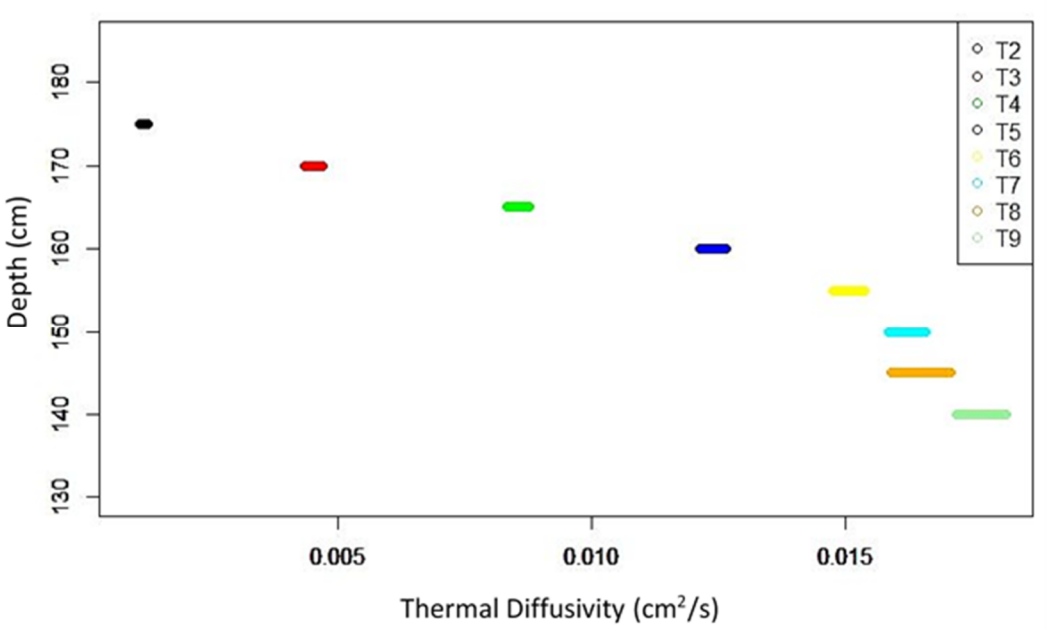

Figure 2.5 – Vertical profile of calculated Ke values within the sediment column for the pea pebble with 50% sand saturation experiment.

2.3.5 Pea Pebble with 75% Sand Saturation

The Pea Pebble with a 3.2 percent sand fraction had an average Ke of 0.010 cm^2/s. The Ke varied between each sensor with a minimum of 0.0019 cm^2/s and a maximum of 0.015 cm^2/s. The maximum and minimum thermal diffusivities occurred at sensor 9, approximately 38.5 cm below the sediment-water interface, and sensor 2, approximately 3.5 cm below the sediment-water interface, respectively. The Ke value was the lowest near the surface of the sediment column and tended to get larger deeper into the sediment column. The measured porosity was 0.43 and that calculated with Wooster et. al.'s equations (2008) was 0.482.

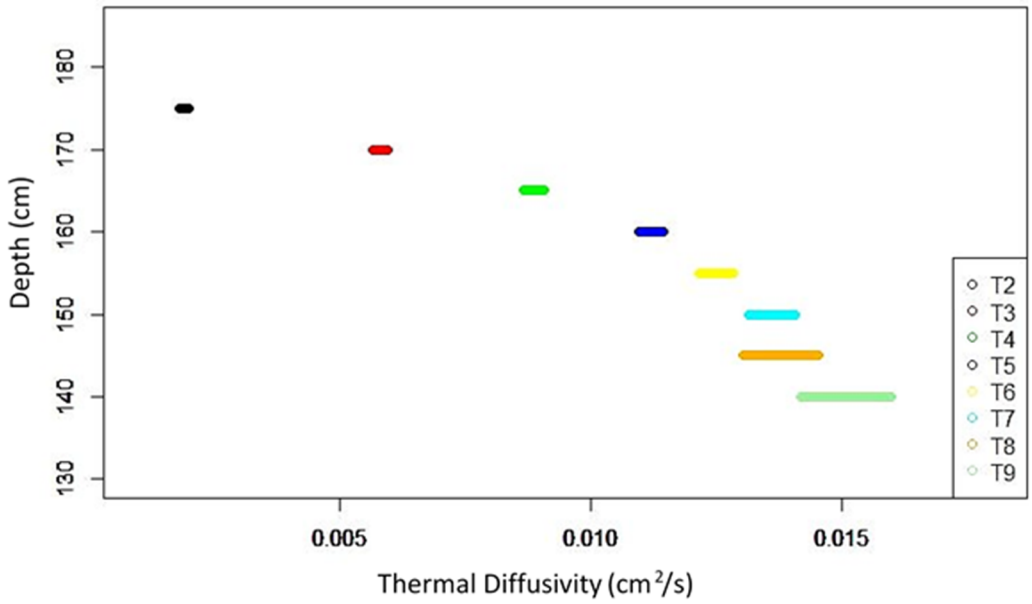

Figure 2.6 – Vertical profile of calculated Ke values within the sediment column for the pea pebble with 75% sand saturation experiment.

2.3.6 Pea Pebble with 100% Sand saturations

The Pea Pebble with a 100% sand saturation of the interstitial pore of the gravel matrix, had an average Ke of 0.0071 cm^2/s. The Ke varied between each sensor with a minimum of 0.0013 cm^2/s and a maximum of 0.014 cm^2/s. The maximum and minimum thermal diffusivities occurred at sensor 9, approximately 38.5 cm from the top of the sediment column, and sensor 2, approximately 3.5 cm from the top of the sediment column, respectively. The Ke value was the lowest near the surface of the sediment column and tended to get larger deeper into the sediment column. The measured porosity was 0.50 and that calculated with Wooster et. al.'s equation (2008) was 0.477.

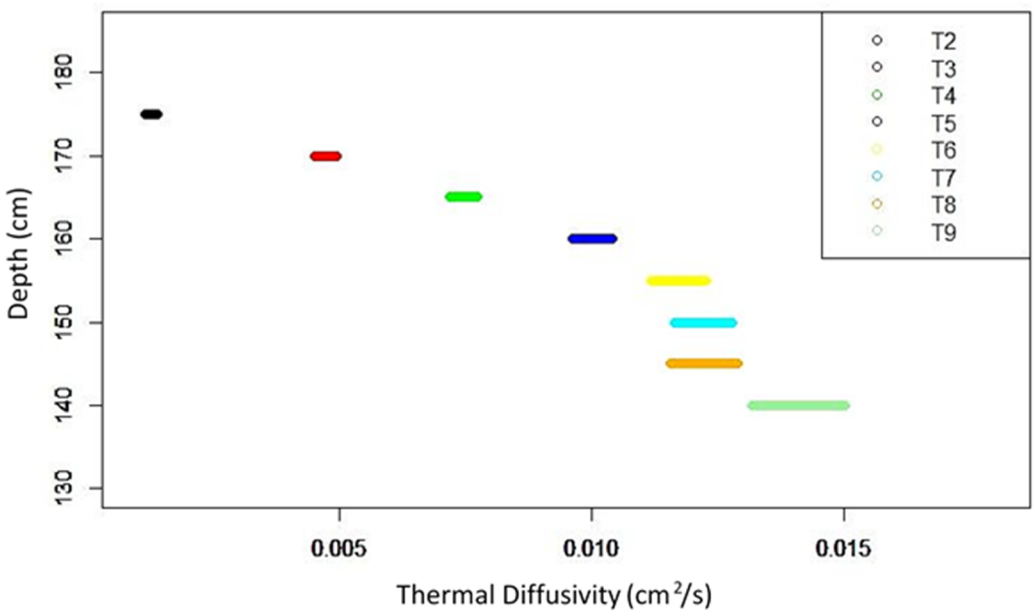

Figure 2.7 – Vertical profile of calculated Ke values within the sediment column for the pea pebble with 100% sand saturation experiment.

2.3.7 Pure Sand

The pure sand test using the temperature sensors had an average Ke of 0.0073 cm^2/s. The Ke varied between each sensor with a minimum of 0.0062 cm^2/s and a maximum of 0.0080 cm^2/s. The maximum and minimum thermal diffusivities occurred at sensor 4, approximately 18.1 cm below the sediment-water interface, and sensor 2, approximately 3.1 cm below the sediment-water interface, respectively. The signal was the lowest near the surface of the sediment column and tended to get larger deeper into the sediment column and became consistent out near the center of the sediment column. The measured porosity was 0.36 and that quantified with Wooster et al.'s equation (2008) was 0.210.

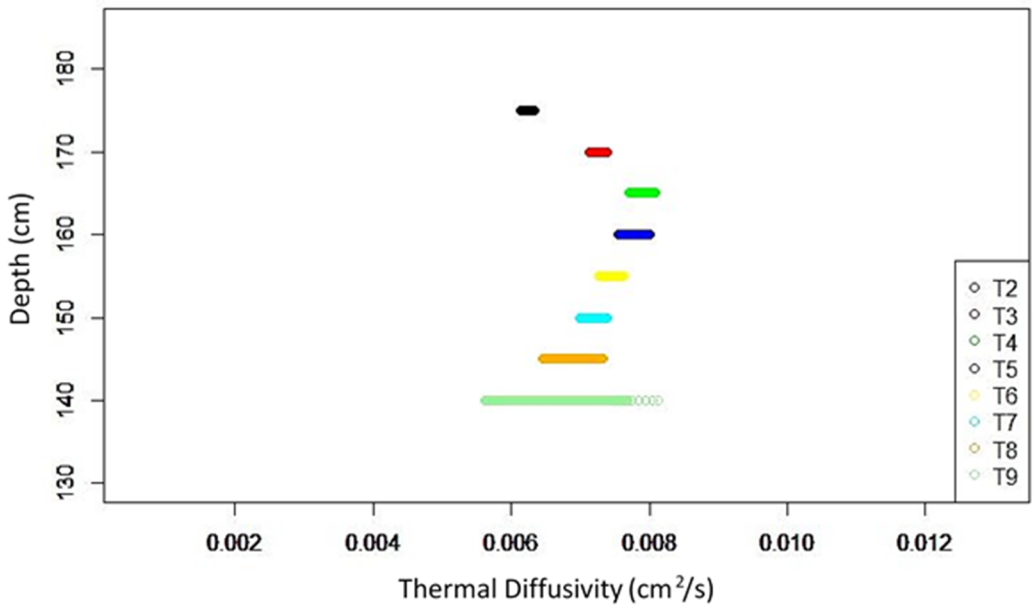

Figure 2.8 – Vertical profile of calculated Ke values within the sediment column for the pure sand experiment.

2.3.8 River Rock with Sand Infiltration

The surface elevation of the sand was measured to have not changed. The average Ke of the system 0.010 cm^2/s. The Ke was largest at the first sensor in the sediment approximately 3.5 cm below the sediment-water interface, with a value of 0.023 cm^2/s. The Ke decreases near the surface and became consistent at approximately 0.0077 cm^2/s at 28.5 cm below the sediment-water interface. The Ke remained roughly constant throughout the rest of the sediment column. There was no visible difference in the Ke between the sand and the river rock. The sand infiltration depth varied throughout the sediment column and did not visibly change from the start of the experiment to the end of data collection.

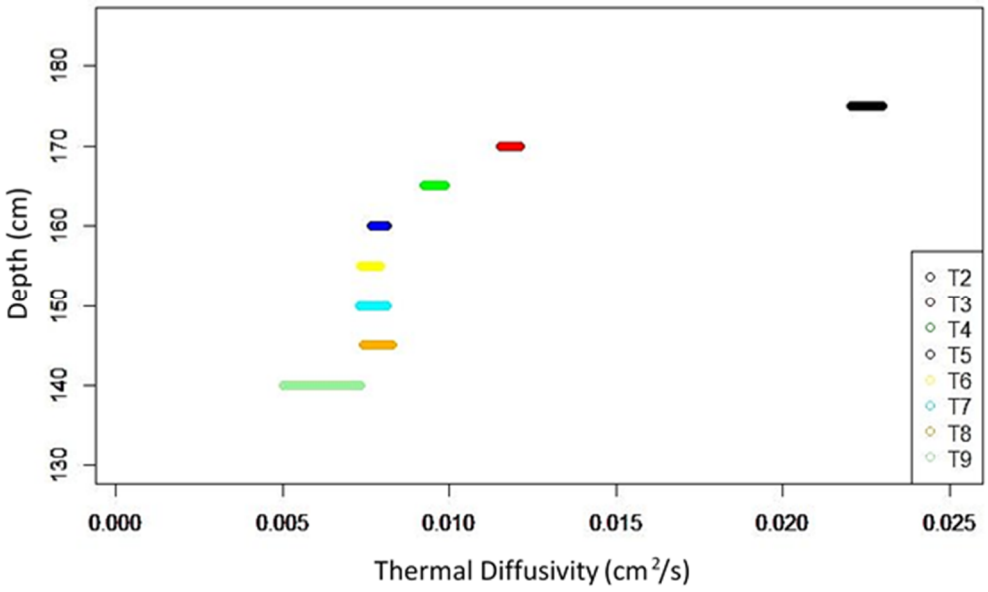

Figure 2.9 – Vertical profile of calculated Ke values within the sediment column for the river rock with sand infiltration experiment.

2.3.9 Comparison of Sediment Compositions

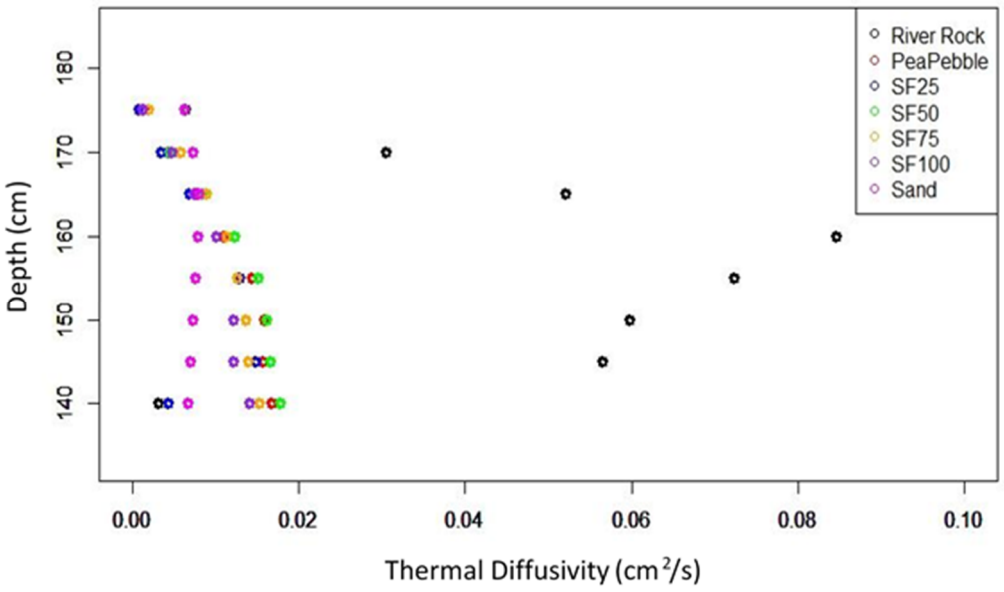

Figure 2.10 – Comparison of the vertical profiles of average Ke values for each experiment.

Ke variations were bounded between river rock (the highest) and pure sand (the lowest), with the other experiments varying between (Figure 2.10). The pea pebble, pea pebble with added

sand, and clean sand compositions had a Ke lower than 0.02 cm^2/s, while the river rock had a Ke of more than three times the rest of the sediment compositions. For all sediment compositions, except for river rock, the Ke began to become constant the further away from the sediment-water interface.

The calculated porosity of the sediment compositions, using Equation 3, varies from 0.21 (pure sand) to 0.50 (pea pebble), while the measured porosity ranges from 0.30 (sand) to 0.50 (pea pebble) (**Table 2.1**). The largest difference between the measured and calculated porosity is 0.15 for sand. The pea pebble and pea pebble with sand fraction tests had a measured porosity within ±0.020 of each other and a calculated porosity within ±0.21 of each other. Median grain sizes of the sediment were 0.3, 4.18, and 15.5 mm for the sand, pea pebbles, and river rock, respectively. The pea pebbles were angular, while the river rock and sand were smooth.

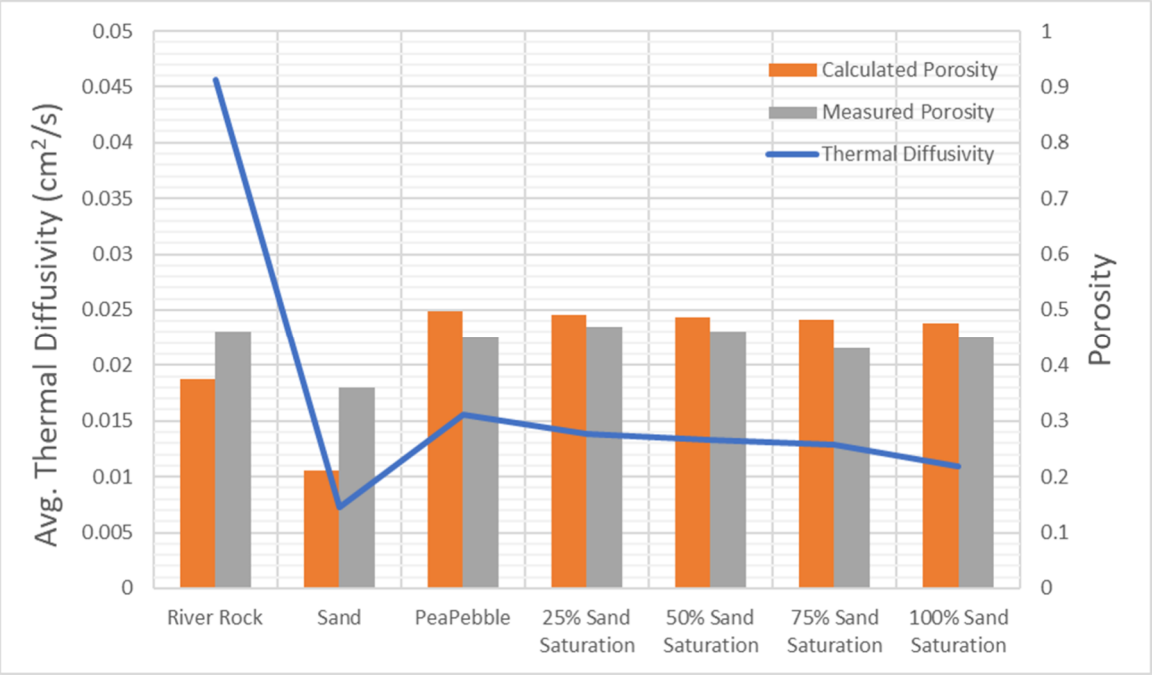

Figure 2.11 – Average Ke values and porosity for each sediment type.

The average Ke of the bottom 20 cm, where the Ke trended toward becoming constant, was compared with porosities of the different sediment compositions (**Figure 2.11**). Sand had the lowest Ke and the lowest porosity. The river rock had highest Ke but the second lowest porosity, while the pea pebble and pea pebble with added sand had the largest porosities and Ke that was between sand and river rock. Although there was not a large difference in the porosities or Ke of the pea pebble and pea pebble with sand, as more sand was added to the sediment composition the Ke decreased.

The Ke decreased by 0.005 cm^2/s or 30% between clean pea pebble and sand saturated pea pebble (100% sand saturation).

2.4 Discussion

Effective thermal diffusion is comprised of two terms. The first term depends only on the thermal diffusion of water and the solids, and the second term accounts for dispersion within the interstitial pores. The latter may be important for large pores and when velocity in the sediment column is fast. When the dispersion component is negligible, then the effective thermal diffusivity (Ke) should range from 0.0014 cm^2/s for water (porosity=1) to 0.019 cm^2/s for solid rock with no voids (porosity=0). A common porosity of 0.32 for a sediment composition has a Ke value of 0.0112 cm^2/s. Estimated Ke values of the river rock in this study were much higher than 0.0112 cm^2/s and close to the end of the Ke range, when porosity is near 0. The high porosity (0.46) of the river rock suggests that dispersion is also an important process for coarse grain material, with large pores, because pores size scales with the median grain size, especially in well sorted material. The river rock with sand clogging from experiment had Ke values within the expected range suggesting that addition of sand reduces the thermal dispersion and thus interstitial velocity and pore size are both low.

Conversely, the experiments with well sorted sand had a value (0.0073 cm^2/s) near those expected for sediment with a porosity of 0.44, which is higher than that estimated from the measured porosity (0.36). This lower value could be due to some accumulation of gasses, which could have been trapped in the sediment column. Air does not absorb heat and therefore would cause the signal to not dampen as much as if air were not present, leading to a higher Ke of the sand. Presence of trapped gasses in the streambed, especially fine sediment(<2mm), is not uncommon. Air bubbles with their higher Ke may increase the Ke of the sediment.

Saturation of the interstitial spaces between gravel with sand resulted in a small difference in Ke. It was expected that the reduction of porosity would have increased Ke allowing the detection of clogging; however, the variation was small and seemed to get lower with porosity. One of the reasons for the contrasting results could be that the material did not compact fully and remained loose. This confirmed what others have observed, perturbation of the streambed material could have important effects on their thermal properties. Gariglio et al. (2013) and Tonina et al. (2014) reported that Ke varied over a one-week period after installation to reach undisturbed conditions.

Another aspect that could have affected the results of Ke is the difficulty to precisely control the velocity through the sediment column. A change in the imposed downwelling velocity among experiments would impact the dispersion component of the Ke of the sediment. The head drop between experiments was closely monitored and held at constant elevation to control the downwelling velocity. The head drop between the water level in the tank and the outlet pipe was set at approximately 0.0018 cm/s, measured by a tipping bucket. The velocity was averaged over the duration of each experiment and was within ±0.003 cm/s between all experiments. Although the range of velocity was minimal between experiments, the uncertainty of the velocity between experiments was 0.002 cm/s or double the imposed velocity. In the field, changes in downwelling velocity may be much larger than the range of variability observed here. Potentially, a more accurate apparatus could improve the results. Additionally, downwelling velocity through the sediment was not constant but changed temporally. This variability in the downwelling velocity could be due to an increase in temperature of the water with warmer water increasing the hydraulic conductivity of the sediment.

In most experiments, a vertical profile of Ke was observed to change with depth in the first 15-20 cm and become nearly constant below the 20 cm. This suggests that vertical changes are limited to the near surface layer. The vertical profile showed two intriguing trends that we were not expected results. In all the experiments with pre-mixed material, Ke increases with depth and reaches a constant value below the first 15-20 cm. Conversely, for the case with sand infiltrating from the top into the clean river rock, Ke decreased with depth. For the latter case, it was hypothesized that this could be due to small air bubbles trapped within the sand. For the former case, it was hypothesized that this could be due to dispersion of the larger grain size material.

Some vertical changes were expected because of sediment stratification that may cause changes in porosity. Stratification was observed in the sand test when layers of the fine sand would lie on top of the coarser sand particles. This could also contribute to the inconsistent Ke profile throughout the sediment column. As sediment is placed into the tank, the different sized particles may fall at a different rate and separate causing stratification, thus changing the thermal properties of the sediment. To reduce stratification, the material could be placed into the empty tank when damp or slightly saturated. When the sediment is damp it allows the particles to stick together, reducing the amount of separation of the sediment when the tank is filled.

In the fine sediment infiltration test, few fine particles infiltrated deeper than one to two centimeters into the coarse grain sizes because of mechanical trapping. At the end of the experiment, it was noticed that moving the sand caused a fair amount of air or gas bubbles to be released from the sediment. Once the bubbles were released sand would fall into the voids of the river rock. The trapped gas bubbles appeared to cause a lower Ke as well as preventing the infiltration of sand into the coarser gravel. To see a more natural infiltration into the sediment, the gravel experiment would need to be run for an extended period of time to allow the sediment to settle and release the trapped gas.

2.5 Conclusion

Results show that monitoring Ke values may not be sufficiently sensitive to detect fine sediment infiltration in fine gravel, like the pea gravel with d_{50}= 4.18 mm, but sufficient in clean and coarse gravel, like the river rock with d_{50}= 15.5 mm. Sand clogging of river rock from a top deposition had a Ke vertical profile opposite to that of sediment composed by uniform mixture of coarse and fine sediments. Thus, the method could be used to discriminate between poorly- and well- sorted coarse sediment, which may help to better manage benthic and hyporheic species.

Values of Ke did not follow the expected trend, with larger values for sediments with low porosity and smaller values for sediments with high porosity. Clean sand (porosity of 0.37) had the lowest Ke and the river rock (porosity of 0.46) had the largest Ke with similar bulk downwelling velocity. Values of Ke were expected to increase with sand fraction in the pea pebble (porosity decreased), but Ke values slightly decreased with sand fraction. This is because Ke values are also sensitive to conditions within the sediments such as trapped gas (air) bubbles, stratification, compaction, and interstitial fluid velocity. Trapped gasses had a noticeable impact on the Ke for the clean sand test, when several gas bubbles were observed to form throughout the experiment. Air and other gasses have a higher Ke than water and sediments, which strongly impact the bulk Ke of the matrix. Mechanical dispersion had the greatest effect on Ke values for the coarsest gravels, which had the highest porosity of 0.46 and largest pore sizes.

The velocity varied among experiments by 0.0012 cm/s primarily due to the difficulty to precisely control the velocity. The change in imposed mean velocity impacts the dispersion component of Ke. Although, the head drop was carefully controlled, small changes in the head drop caused differences in the imposed mean velocity. Since the velocity was not the same among

experiments, this may have partially impacted Ke values. To improve the accuracy of the experiment, a more precise mechanism for controlling the imposed mean velocity should be adopted.

This suggests that Ke values are more influenced by interstitial flow velocity than the composition or porosity of the sediment for poorly sorted or fine gravel. The velocity may cause major differences in heat transport and thus in Ke values. In field applications, the interstitial velocities may vary widely and cause variable changes to Ke values.

REFERENCES CITED

Anderson, N., Ismael, A., & Thitimakorn, T. (2007). Ground-penetrating radar; a tool for monitoring bridge scour. Environmental & Engineering Geoscience, 13(1):1-10.

Avent, R.R., & M. Alawady. (2005). Bridge scour and substructure deterioration: case study. Journal of Bridge Engineering, 10:247-254.

Chen, G., Schafer, P.B., Zhibin, L., Huang, Y., Suaznabar, O., Shen, J., & Kerenyi, K. (2015). Maximum scour depth based on magnetic field change in smart rocks for foundation stability evaluation of bridges. Structural Health Monitoring, 14(1):86-99.

Constantz, J. (1998). Interaction between stream temperature, streamflow, and groundwater exchanges in alpine streams. Water Resources Research, 34(7):1609-15. doi:10.1029/98WR00998.

Cui, Y., Wooster, J.K., Baker, P.F., Dusterhoff, S.R., Sklar, L.S., & Dietrich W.E. (2008). Theory of Fine Sediment Infiltration into Immobile Gravel bed. Journal of Hydraulic Engineering, 134(10): 1421-1429. doi: 10.1061/(ASCE)0733-9429(2008)

Datry, T., Lamouroux, N., Thivin, G., Descloux, S., & Baudoin, J.M. (2015). Estimation of sediment hydraulic conductivity in river reaches and its potential use to evaluate streambed clogging, River Research Applications, 31:880-891. doi: 10.1002/rra.

De Falco, F., & Mele, R. (2002). The monitoring of bridges for scour by sonar and sedimetri. NDT&E International, 35(2):117-123.

DeWeese, T. (2015). Monitoring streambed scour/deposition using non-sinusoidal water temperature signals and during flood events. M.S. Thesis, Department of Civil Engineering, University of Idaho. (40 pp.)

Einstein, H.A. (1968). Deposition of suspended particles in a gravel bed. Journal of the Hydraulics Division, 94(5):1197-1205.

Fisher, A.M., & Khan, A. (2013). A novel vibration-based monitoring technique for bridge pier and abutment scour. Structural Health Monitoring, 12(2):114-125.

Forde, M.C., McCann, D.M., Clark, M.R., Broughton, K.J., Fenning, P.J., & Brown, A. (1999). Radar measurement of bridge scour." NDT&E International, 32:481-492.

Foti, S., & Sabia, D. (2011). Influence of foundation scour on the dynamic response of existing bridge. Journal of Bridge Engineering, 16(2):295-304.

Geig, S.M., Sear, D.A., Carling, P.A. (2005). The impact of fine sediment accumulation on the survival of incubating salmon progeny: Implications for sediment management, Science of The Total Environment, 344(1-3):241-258.

Hatch, C.E., Fisher, A.T., Revenaugh, J.S., Constantz, J., & Ruehl, C.. (2006). Quantifying surface water-groundwater interactions using time series analysis of streambed thermal records: method development. Water Resources Research, 42(10):1-14. doi:10.1029/2005WR004787.

Hayden, J.T., & Puleo, J.A. (2011). Near real-time scour monitoring system: Application to Indian River Inlet, Delaware. Journal of Hydraulic Engineering, 137(9):1037-1046.

Horne, W.A. (1993). ‘Scour Inspection using Ground Penetrating Radar’, Proceedings of National Conference on Hydraulic Engineering, San Francisco, CA, 1993. pp. 1888-1893.

Hunt, B.E. (2009). Monitoring Scour Critical Bridges: A Synthesis of Highway Practice. NCHRP Synthesis 396. Transportation Research Board. National Academy of Science, Washington, D.C. [Google Books version]. books.google.com/books?id=f0-ZPJFgSsEC&pg=PP3&lpg=PP3&dq=Hunt,+B.E.+(2009).+Monitoring+Scour+Critical+Bridges:+A+Synthesis+of+Highway+Practice.+NCHRP+Synthesis+396.+Transportation+Research+Board.+National+Academy+of+Science,+Washington,+D.C.&source=bl&ots=Uq0-FearVM&sig=ACfU3U2EzWjqwnwtf-C4eoPWKzJDHOxhCQ&hl=en&sa=X&ved=2ahUKEwjhnsbHkMHpAhXIITQIHQe8CeAQ6AEwAnoECAoQAQ#v=onepage&q&f=false

Idaho Transportation Department. (2004). Field Manual. Scour Critical Bridges: High-Flow Monitoring and Emergency Procedures. https://www.fhwa.dot.gov/engineering/hydraulics/pubs/idfieldpoa.pdf

Idaho Transportation Department. (2016). Idaho Manual for Bridge Evaluation. http://apps.itd.idaho.gov/apps/bridge/manual/IMBE2016.pdf

Junliang, T., Yu, X., & Yu, X. (2013). 'Real-time TDR field bridge scour monitoring system', Structures Congress 2013: Bridging Your Passion with Your Profession. Pittsburg, PN, 2-4 May 2013. pp. 2996-3009.

Kamojjala, S., Gattu, N.P., Parola, A.C., & Hagerty, D.J. 1994. Analysis of 1993 Upper Mississippi flood highway infrastructure damage. *In:* Proceedings of the 1st International Conference of Water Resource Engineering. New York: American Society of Civil Engineers 1994, pp. 1061-1065.

Katsui, H., & Toue, T. (1993). Methodology of estimation of scouring around large-scale offshore structures, Proceedings of the 3rd International offshore and Polar Engineering Conference, Singapore, 6-11 June 1993. Vol. 1, pp. 599-602.

Keery, J., Binley, A., Crook, N., & Smith, J.W.N.. (2007). Temporal and spatial variability of groundwater-surface water fluxes: development and application of an analytical method using temperature time series. Journal of Hydrology, 336(1):1-16. doi:10.1016/j.jhydrol.2006.12.003

Kenney, T. A., & McKinney, T. S. (2006). Hydraulic and Geomorphic Monitoring of Experimental Bridge Scour Mitigation at Selected Bridges in Utah, 2003-05. Salt Lake City, UT: United States Geological Survey. https://pubs.usgs.gov/sir/2006/5033/PDF/sir2006_5033.pdf

Lautz, L.K. (2012). Observing temporal patterns of vertical flux through streambed sediments using time-series analysis of temperature records. Journal of Hydrology, 464-465:199-215. doi:10.1016/j.jhydrol.2012.07.006.

Lee, S., & Sturm, T. (2009). Effect of sediment size scaling on physical modeling of bridge pier scour. Journal of Hydraulic Engineering, 135(10):793-802.

Lin, Y.B., Lai, J.S., Chang, W.Y., Lee, F.Z., & Tan, Y.C. (2010). Using mems sensors in the bridge scour monitoring system. Journal of the Chinese Institute of Engineers, 33(1):25-35.

Luce, C.H., Tonina, D., Gariglio, F., & Applebee, R. (2013). Solutions for the diurnally forced advection-diffusion equation to estimate bulk fluid velocity and diffusivity in streambeds from temperature time series. Water Resources Research, 49(1):488-506. doi:10.1029/2012WR012380.

Nichol, D., & Reynolds J.M. (1999). Ground penetrating radar survey to detect scour holes beneath the A525 highway at Nant-y-Garth, Wales: a case history. Quarterly Journal of Engineering Geology, 32:157-162.

Nogaro, G., Datry, T., Mermillod-Blondin, F., Descloux, S., & Montuelle, B. (2010). Influence of streambed sediment clogging on microbial processes in the hyporheic zone, Freshwater Biology. Black well Publishing Ltd, 55: 1288-1302. doi:10.111/j.365-2427.2009.02352.x

Platts, W.S., Shirazi, M.A., & Lewis, D.H., (1979). Sediment particle sizes used by salmon for spawning with methods for evaluation, Environmental Protection Agency. EPA-600/33-79-O43.

Prendergast, L.J., & Gavin, K. (2014). A review of bridge scour monitoring techniques. Journal of Rock Mechanics and Geotechnical Engineering, 6:138-149.

Rabení, C.F., Doise, K.E., & Zweig, L.D., (2005). Stream invertebrate community functional responses to deposited sediment. Aquatic Science 67: 395-402. doi: 10.1007/s0027-005-0793-2.

"Researchers Test Low-Cost Thermal Method to Monitor Bridge Scour." Blog post. The Transporter. Idaho Transportation Department, 13 Mar. 2015. Web. 25 Apr. 2017. <http://apps.itd.idaho.gov/apps/MediaManagerMVC/transporter/2015/032015_Trans/032015_BridgeScourStory.html>.

Richardson, E.V. (1999). History of Bridge Scour Research and Evaluations Paper: History of Bridge Scour Research and Evaluation in the United States. In E.V. Richardson & P.F. Lagasse (Eds.), *Stream Stability and Scour at Highway Bridges*: *A Compendium of Papers, ASCE Water Resources Engineering Conferences 1991 to 1998* (pp. 15-40). Reston, VA: American Society of Civil Engineers. [Google Books version]. https://books.google.com/books?id=yihA7rihpicC&pg=PA765&lpg=PA765&dq=Lagasse,+P.F.,+Schall,+J.K.,+Johnson,+F.,+Richardson,+E.V.,+%26+Chang,+F.+(1995).+Stream+Stability+at+Highway+Structures.+Washington,+D.C.&source=bl&ots=uBMk9aR9_N&sig=ACfU3U3lW77unquowlFd6-zitgXhva0lg&hl=en&sa=X&ved=2ahUKEwjgr626lMHpAhV_JzQIHfMRAJEQ6AEwAHoECAoQAQ#v=onepage&q=60%20percent&f=false

Saito, E., Sato, S., & Shibayama, T. (1990). 'Local scour around a large circular cylinder due to wave action', Proceedings of Coastal Engineering Conference, Delft, Netherlands 2-6 July 1990.

Schälchli, U. (1992). The clogging of coarse gravel river beds by fine sediment, Hydrobiologia, 235(236):189-197.

Sohn, H., Farrar, C.R., Hermez, F., & Czarnecki, J. (2004). A Review of Structural Health Monitoring Literature: 1996-2001. Los Alamos National Laboratory, 311 pp.

Sumer, B. M., & Fredsoe, J. (2001). Scour around pile in combined waves and current. Journal of Hydraulic Engineering, 127(5).

Swanson, T.E., & Bayani Cardenas, M. (2010). Diel heat transport within the hyporheic zone of a pool-riffle-pool sequence of a losing stream and evaluation of models for fluid flux estimation using heat. Limnology and Oceanography, 55(4):1741-54. doi:10.4319/lo.2010.55.4.174

Tao, J., Yu, X., & Yu, X. (2013). Real-time Field Bridge Scour Monitoring System. 2013 ASCE Structures Congress.

Tonina, D., Luce, C., & Gariglio, F. (2014). Quantifying streambed deposition and scour from stream and hyporheic water temperature time series. Water Resources Research, 50(1):287-292. doi:10.1002/2013WR014567.

Topczewski, L., Ciesla, J., Mikolajewski, P., Admaski, P., & Markowski, Z. (2016). Monitoring of scour around bridge piers and abutments. Transportation Research Procedia, 14:3963-3971.

Webb, D.J., Anderson, N.L., Newton, T. & Cardimona, S. (2000). Bridge Scour: Application of Ground Penetrating Radar. Federal Highway Administration and Missouri Department of Transportation Special Publication.

Wooster, J. K., Dusterhoff, S., Cui, Y., Sklar, L. S., Dietrich, W. E., & Malko, M. (2008). Sediment supply and relative size distribution effects on fine sediment infiltration into immobile gravels. Water Resources Research, 44, W03424.

Yao, C., Darby, C., Hurlebaus, S., Price, G., Sharma, H., Hunt, B., & Briaud, J.-L. (2010). 'Scour Monitoring Development for two Bridges in Texas', International Conference on Scour and Erosion 2010. San Francisco, CA, 7-10 November 2010. American Society of Civil Engineers. pp 958-967.

Zarafshan, A., Iranmanesh, A., & Ansari, F. (2012). Vibration-based method and sensor for monitoring of bridge scour. Journal of Bridge Engineering, 17(6):829-838.

APPENDIX A: FINE SEDIMENT FRACTION CALCULATION

Determine the fine sediment fraction by volume using the grain size distribution curves and the amount of sand added for each successive experiment.

Produced By: Aston Carpenter

Variables:

s = sand
g = pea pebbles
V = Volume
Vt = Total volume in Tank
fs = saturated fine sediment fraction
W = Weight in kg
Fs = Fine Sediment Fraction by Volume

Porosity:

$\lambda s := 0.361$ Sand

$\lambda g := 0.441$ Pea Pebbles

Geometric mean grain size:

$Dsg := 0.407 \quad mm$

$Dgg := 5 \quad mm$

Particle Density:

$\rho g := 2521.32 \ \frac{kg}{m^3}$

$\rho s := 2109.64 \ \frac{kg}{m^3}$

Equations:

Fs = Vs/Vt
Vs = Ws/ ρs

Weight and Volume of Pea Pebbles:

$Vt := 0.0731 \quad m^3$ $Wg := 104.65 \quad kg$ $Vg := (1 - \lambda g) \cdot Vt = 0.041 \quad m^3$

$Vvoids := Vt \cdot \lambda g = 0.032 \quad m^3$ With no added sand.

Experiment 1: Calculation of Fraction of Fine Sediment Fraction for 0.91 kg of sand added to Pea Pebbles

Weight and volume of sand added:

$Ws1 := 0.91 \quad kg$ $Vs1 := \frac{Ws1}{\rho s} = 4.314 \cdot 10^{-4} \ m^3$

Solve for Fine Sediment Fraction and total sediment fraction

$Fs1 := \frac{Vs1}{Vg} \cdot 100 = 1.056\%$

Experiment 2: Calculation of Fraction of Fine Sediment Fraction for 1.82 kg of sand added to Pea Pebbles

Weight and volume of sand added:

$Ws2 := 1.82 \quad kg$ $\qquad Vs2 := \frac{Ws2}{\rho s} = 8.627 \cdot 10^{-4} \ m^3$

Solve for Fine Sediment Fraction and total sediment fraction

$Fs2 := \frac{Vs2}{Vg} \cdot 100 = 2.111\%$

Experiment 3: Calculation of Fraction of Fine Sediment Fraction for 1.82 kg of sand added to Pea Pebbles

Weight and volume of sand added:

$Ws3 := 2.73 \quad kg$ $\qquad Vs3 := \frac{Ws3}{\rho s} = 0.001$

Solve for Fine Sediment Fraction and total sediment fraction

$Fs3 := \frac{Vs3}{Vg} \cdot 100 = 3.167\%$

Experiment 4: Calculation of Fraction of Fine Sediment Fraction for 3.64 kg of sand added to Pea Pebbles

Weight and volume of sand added:

$Ws4 := 3.64 \quad kg$ $\qquad Vs4 := \frac{Ws4}{\rho s} = 0.002$

Solve for Fine Sediment Fraction and total sediment fraction

$Fs4 := \frac{Vs4}{Vg} \cdot 100 = 4.222\%$

Calculation of the saturated Fine Sediment Fraction (FSF) for the Sand Infiltration Experiment, using equation 4 from Wooster et. al., 2008.

Porosity:

$\lambda s := 0.361$ Sand

$\lambda g := 0.46$ River Rock

Geometric mean grain size:

$Dsg := 0.407$ mm

$Dgg := 15.17$ mm

Standard deviation

$$\sigma sg := \left(1.61 \cdot \lambda s\right)^{-1.517} = 2.278$$

$$\sigma gg := \left(1.61 \cdot \lambda g\right)^{-1.517} = 1.577$$

Calculation of saturated fine sediment fraction

$$fs := \left(\frac{0.621 \cdot \left(1 - 0.621 \cdot \sigma sg^{-0.659}\right) \cdot \sigma gg^{-0.659}}{1 - 0.621^2 \cdot \left(\sigma sg \cdot \sigma gg\right)^{-0.659}}\right) \cdot \left(1 - \exp\left(-0.0146 \cdot \left(\frac{Dgg}{Dsg}\right) + 0.0117\right)\right)$$

$$fs = 0.146$$